A&A 539, A19 (2012)
DOI: 10.1051/0004-6361/201118491

Astronomy & Astrophysics

The Na-O anticorrelation in horizontal branch stars

II. NGC 1851⋆

R. G. Gratton[1], S. Lucatello[1], E. Carretta[2], A. Bragaglia[2], V. D'Orazi[1], Y. Al Momany[1,3], A. Sollima[1], M. Salaris[4], and S. Cassisi[5]

[1] INAF-Osservatorio Astronomico di Padova, Vicolo dell'Osservatorio 5, 35122 Padova, Italy
e-mail: raffaele.gratton@oapd.inaf.it
[2] INAF-Osservatorio Astronomico di Bologna, via Ranzani 1, 40127 Bologna, Italy
[3] European Southern Observatory, Alonso de Cordova 3107, Vitacura, Santiago, Chile
[4] Astrophysics Research Institute, Liverpool John Moores University, UK
[5] INAF-Osservatorio Astronomico di Teramo, via Collurania, Teramo, Italy

Received 21 November 2011 / Accepted 7 December 2011

ABSTRACT

The chemical composition of horizontal branch (HB) stars might help to clarify the formation history of individual globular clusters (GCs). We studied the Na-O anti-correlation from moderately high resolution spectra for 91 stars on the bimodal HB of NGC 1851; in addition we observed 13 stars on the lower red giant branch (RGB). In our HB sample, 35 stars are on the blue HB (BHB), one is an RR Lyrae, and 55 stars are on the red HB (RHB). The ratio of BHB to RHB stars is close to the total in the cluster (35 and 54%, respectively), while RR Lyrae variables are under-represented, (they are ∼12% of the NGC 1851 stars). We also derived abundances for He and N in BHB stars. For RHB stars we derived Ba abundances and a few interesting upper limits for N. The RHB stars clearly separate into two groups: the vast majority are O-rich and Na-poor, while about 10–15% are Na-rich and moderately O-poor. Most (but not all) Na-rich RHB stars are also Ba-rich and there is an overall correlation between Na and Ba abundances within the RHB. The group of Ba-rich RHB stars resides on the warmer edge and includes ∼10% of the RHB stars. We propose that they are the descendant of the stars on the RGB sequence with very red $v - y$ colour. This sequence is known also to consist of Ba and perhaps CNO-rich stars and consistently includes ∼5–10% of the RGB stars of NGC 1851. However, the upper limit we obtain for N ([N/Fe] < 1.55) for one of the Ba-rich stars coupled with the low C-abundances for RGB Ba-rich stars from the literature suggests that the total CNO might not be particularly high ([(C+N+O)/Fe] ≤ 0.15). The other Na-rich RHB stars are also at the warm edge of the RHB and the only RR Lyrae is Na-rich and moderately O-poor. We also find a Na-O anticorrelation among BHB stars, partially overlapping that found among RHB stars, though generally BHB stars are more Na-rich and O-poor. However, there is no clear correlation between temperature and Na and O abundances within the BHB. The average He abundance in BHB stars is $Y = 0.29 \pm 0.05$, which excludes a large population of extremely He-rich stars from our sample. N abundances are quite uniform at [N/Fe] = 1.16 ± 0.14 among BHB stars, with a small trend with temperature. This value is consistent with normal CNO abundance and excludes that BHB stars are very CNO-rich: this leaves an age spread of ∼1.5 Gyr as the only viable explanation for the split of the SGB. To help clarifying the formation history of NGC 1851, we computed synthetic HB's trying to identify which HB stars are the descendant of the bright and faint subgiant branch (b-SGB and f-SGB) stars identified by Milone et al. (2008, ApJ, 673, 241), with respectively 2/3 and 1/3 of the stars of NGC 1851. While most BHB stars likely descend from f-SGB stars and are older, and most RHB stars from b-SGB ones and are younger, the correspondence is probably not one-to-one. In particular, the Ba-rich RHB stars should be less massive than the remaining RHB stars, and the location of their progenitors on the SGB is uncertain. If they descend from f-SGB stars, number counts then require that RR Lyrae variables and possibly some mild BHB stars descend from b-SGB stars; this suggestion is supported by a few circumstantial facts. An investigation of the composition of a large enough sample of SGB stars is required to firmly establish these relations.

Key words. stars: evolution – stars: abundances – stars: Population II – globular clusters: general – globular clusters: individual: NGC 1851

1. Introduction

The distribution of stars along the horizontal branch (HB) of globular clusters (GC) provides a wealth of information that can be used to understand their formation and evolution. It is well known that several parameters are required to explain the shape of the HBs (van den Bergh 1967; Sandage & Wildey 1967; see discussion in Gratton et al. 2010), the two most important being the overall metallicity (usually defined by [Fe/H]: Sandage & Wallerstein 1960; Faulkner 1966), and age (see e.g. Dotter et al. 2010). In the recent years, it has become clear that star-to-star variations in He content also play an important role (D'Antona et al. 2002; D'Antona & Caloi 2004; Carretta et al. 2009; Gratton et al. 2010). They are related to the phenomenon of multiple populations (Gratton et al. 2004, 2012; Piotto et al. 2008), that is the presence of several generations of stars in GCs, the ejecta of a fraction of the stars from the earliest one polluting the material from which younger stars formed. Together with He, the abundances of several other elements change, including those produced by p-capture reactions in high-temperature H-burning that can then be used as tracers of this phenomenon. Anti-correlations are expected between C

⋆ Based on observations collected at ESO telescopes under program 386.D-0086.

and N, O and Na, Mg and Al, depending on the temperature at which the H-burning occurred (which in turn is related to the mass of the polluters) and then on the timescale of the whole process. The abundance of these elements may then be used as a powerful diagnostics of the early phases of GC evolution.

Clusters with extended or even discontinuous distribution of stars along the HB (see Catelan et al. 1998) may be particularly interesting. In this general frame, it should be expected that there is an overall correlation between the colour (i.e. temperature) of the stars along the HB and the abundances of He and *p*-capture elements (D'Antona & Caloi 2004). While many circumstantial evidence favour this scenario (see e.g. Gratton et al. 2010, and references therein), few GCs have been studied with adequate data to provide a more direct confirmation. Very recently, the existence of a clear correlation between HB morphology and Na-O anticorrelation have been soundly proved for M4 (Marino et al. 2011) and by our team for NGC 2808 (Gratton et al. 2011). However, data on additional GCs are required because there are other mechanisms that might potentially cause spreads in colours of stars along the HB (spread in mass loss, age, metallicity). For instance, such an effect may be produced by the merging of clusters of different age/chemical composition (van den Bergh 1996; Catelan 1997), a phenomenon that might possibly occur within a dwarf galaxy, later accreted by the Milky Way (Bellazzini et al. 2008; Bekki & Yong 2012). Disentangling the effects of these various mechanisms is basic to a proper understanding of GC formation and evolution.

NGC 1851 is one of the most interesting GCs on this respect. Its HB is very peculiar, with a pronounced bimodal distribution of stars: a red HB (RHB), comprising ~54% of the stars, a blue HB (BHB: ~35%) and quite few RR Lyrae variables (~12%: Walker 1998; Saviane et al. 1998; Milone et al. 2009, who obtained a slightly higher fraction of RHB stars)[1]. While this might be explained by He abundance variations, in analogy with the case of NGC 2808 (D'Antona & Caloi 2004), the blue HB is actually only slightly brighter than the red one, much less than it should be expected for the difference in He content required to explain the large spread in colours (see Salaris et al. 2008). NGC 1851 shows other important differences from NGC 2808. First, the BHB is much shorter, lacking the long blue tail which is very prominent in NGC 2808. This agrees with its much fainter total absolute magnitude, because there is a good correlation between the maximum temperature of the HB stars and cluster luminosity (Recio-Blanco et al. 2006). It is an additional indication that NGC 1851 lacks very He-rich stars, a fact which is also derived from the absence of any discernible split of the MS (Milone et al. 2008). Second, the same Milone et al. (2008) showed that the subgiant branch splits into two sequences, the faint (f-SGB) one including 34 ± 3% of the stars, the remaining being on the brighter one (b-SGB). This splitting might be interpreted either as a spread of age (about 1 Gyr: Milone et al. 2008) or as the f-SGB being overabundant in CNO elements by ~0.3 dex or more (Cassisi et al. 2008; Salaris et al. 2008; Ventura et al. 2009). In the first case, the progeny of the f-SGB could be identified with the BHB, while the b-SGB might correspond to the RHB; the opposite should hold in the second case[2]. The number ratio favours then the first hypothesis, though the abundance analyses discussed below possibly support the second one. Furthermore, Strömgren photometry of RGB stars (Grundahl & Bruntt 2006; Villanova et al. 2009; Carretta et al. 2011a,b) shows a peculiar sequence with very red $v - y$ colours that includes some 5–10% of the stars. This sequence could also be explained by an overabundance of CNO elements (Carretta et al. 2011b); however its relation with the splitting of the SGB and HB is not clear, because the fraction of f-SGB stars is much higher than that of stars on the red $v - y$ RGB sequence.

Various spectroscopic studies of red giants of NGC 1851 have been carried out in the last few years. They provided very interesting results, but not yet a final understanding of this cluster. Yong & Grundahl (2008) and Yong et al. (2009) studied a few stars with high resolution and high S/N spectra. At variance from what is typical of GCs, they found a correlation between *p*-capture and *n*-capture elements, as well as hints for a spread in CNO elements. The correlation between *p*- and *n*-capture elements has been confirmed by Villanova et al. (2010) using a slightly larger sample of stars; they however did not find any spread in CNO elements, possibly because of uncertainties in the transformation from relative to absolute abundances required for this determination (see Yong et al. 2011). They also found that stars on the red $v - y$ sequence are typically Ba-rich. Carretta et al. (2010, 2011) considered a much larger sample of red giants, albeit at lower resolution and S/N. They found a spread in [Fe/H] values larger than typical in GCs, which they interpreted as due to different populations; this agrees with what found from narrow band Ca II photometry (Lee et al. 2009). They also confirmed the correlation between *n*- and *p*-capture elements, and found that Ba-rich stars are typically more metal-rich than average. The stars on the red $v - y$ sequence are indeed Ba-rich, but they found also some Ba-rich stars among the normal sequence (admittedly, these Ba abundances have rather large errors being based on a single, less than optimal line).

The overall pattern of abundances of NGC 1851 is clearly peculiar and cannot easily fit into the scheme adopted for more typical GCs such as M4 or NGC 2808. The only other cluster where a spread of Fe and a correlation between *p*- and *n*-capture elements have been found is M22, if we leave aside the two more massive ones, ω Cen and M54. Developing earlier similar concepts by van den Bergh (1997) and Catelan (1998), Carretta et al. (2010, 2011a) proposed that NGC 1851 is actually the result of the merging of two clusters, each one having their own Na-O anticorrelation, differing in age (by about 1–2 Gyr) and with a small difference in [Fe/H]. In their picture, the f-SGB, the Fe and Ba-poor RGB population, and the BHB are related to the older cluster; and the b-SGB, the Fe and Ba-rich RGB, and the RHB to the young one. Since there are however indications that NGC 1851 hosts also CNO-rich stars, it is possible that some of the f-SGB stars are actually CNO-rich stars of a younger population. In this scheme, there should be a complex correlation between chemical composition and colours of stars along the RHB,

[1] The different radial distribution of RHB and BHB stars within the cluster makes an exact estimate of the relative fractions quite complicate (Saviane et al. 1998; Milone et al. 2008, 2009). Here, we use the fractions derived at rather large distances from the center (typically in the range 2–10 arcmin) because our spectroscopic data mainly sample this region. For comparison, the core and half light radii of NGC 1851 are 0.09 and 0.51 arcmin, respectively (Harris et al. 1996).

[2] While acknowledging the problem related to number counts, Salaris et al. (2008) and Ventura et al. (2009) explored the possibility that a CNO-rich f-SGB coeval with a CNO-normal b-SGB is connected to the BHB. Everything else held constant, CNO-rich HB's should be redder and not bluer than CNO-poor ones. While a corresponding variation in He might result in a bluer HB, the variation proposed by Ventura et al. of $\Delta Y \sim 0.04$ is not enough to justify the proposed connection. With this hypothesis, the only possibility to reconcile models with observations would then be to assume that CNO-rich stars experience a larger mass loss along the RGB.

at variance with the cases for M 4 and NGC 2808. An explicit study of the chemical composition of stars along the HB might then help clarifying which is the correct scenario. In this paper we present the results of such a study.

The structure of the paper is the following: in Sect. 2 we present the observational data; in Sect. 3 we explain our analysis methods; in Sect. 4 we discuss the results of the abundance analysis; conclusions are drawn in Sect. 5.

2. Observation

We acquired spectra for 35 stars on the BHB, 1 RR Lyrae variable[3], 57 stars on the RHB, and 13 on the lower RGB (luminosity below the bump) of NGC 1851 using the GIRAFFE fibre-fed spectrograph at VLT (Pasquini et al. 2004). All stars were chosen to be free from any companion closer than 2 arcsec and brighter than $V + 2$ mag, where V is the target magnitude. The remaining fibres were used to acquire sky spectra. The median spectra from these last fibres were subtracted from those used for the stars. This was of particular relevance here, because the observed stars are typically very faint. We used two spectral configurations: HR12 (spectral range from 5808 to 6138 Å) and HR19 (from 7728 to 8317 Å), providing high resolution spectra including the strongest features of O I (the IR triplet at 7771–74 Å) and Na I (the resonance D doublet at 5890–96 Å, as well as the subordinate strong doublet at 8183–94 Å) accessible from ground and the only ones that might be used to determine O and Na abundances without a prohibitively long observing time. A few lines of N, Mg, Al, Si, Ca, Fe, and Ba were also included in the selected observing ranges. Different fibre configurations were used in order to observe a quite large number of RGB stars with the UVES spectrograph; these observations will be described elsewhere. We have observations with both gratings only for a subset of stars because a change in the UVES fibers placements requires a repositioning also of the GIRAFFE fibers to maximize the number of UVES RGB stars.

Our program was executed in service mode. We obtained a total of 6666 s (3×2222 s exposures) and 7500 s (3×2500 s) of observation with the gratings HR12 and HR19, respectively. The S/N of the summed spectra for the two gratings is typically ~35 and ~60, ~22 and ~32, and ~30 and ~50, for RHB, BHB, and RGB stars, respectively. The spectra were reduced by the ESO personnel using the ESO FLAMES GIRAFFE pipeline version 2.8.7. Sky subtraction, combination of individual exposures for each star, translation to rest-frame and continuum tracing were performed within IRAF[4]. Telluric lines were removed from the longest wavelength spectra by dividing the average spectrum of the warmer BHB stars (those with $T_{\rm eff} > 11\,500$ K). This combined spectrum has a S/N much higher than those of the individual program stars, and was obviously taken with the same airmass, so that the excision of the telluric lines turned out to be excellent. Examples of spectra are shown in Fig. 1.

[3] In our original strategy we avoided observing RR Lyrae because it is difficult to optimize multi-object observations in service mode for variable stars. However, one RR Lyrae star was mistakenly included in the sample. Luckily, all spectra turned out to be taken close to minimum, in the most favourable phase for abundance analysis. This star was then kept in the analysis.

[4] IRAF is distributed by the National Optical Astronomical Observatory, which are operated by the Association of Universities for Research in Astronomy, under contract with the National Science Foundation.

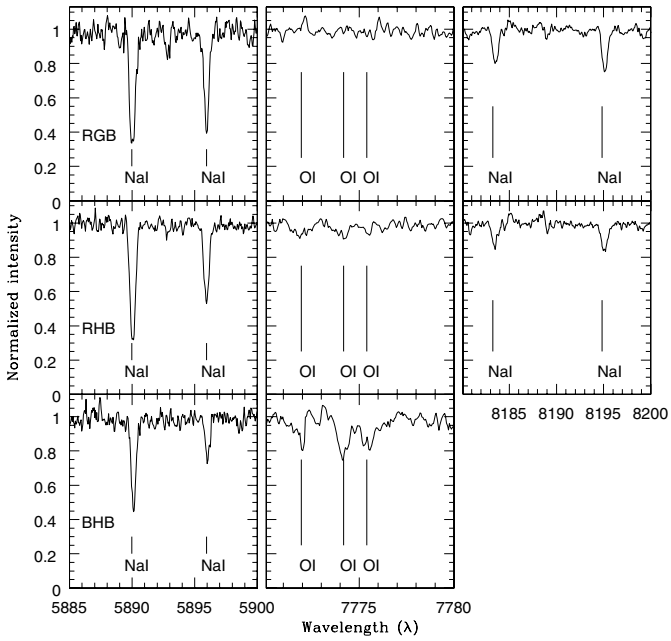

Fig. 1. Portion of the spectra of an RGB star (#50876: *upper row*), a RHB (#22164: *middle row*), and a BHB star (#18358: *bottom row*).

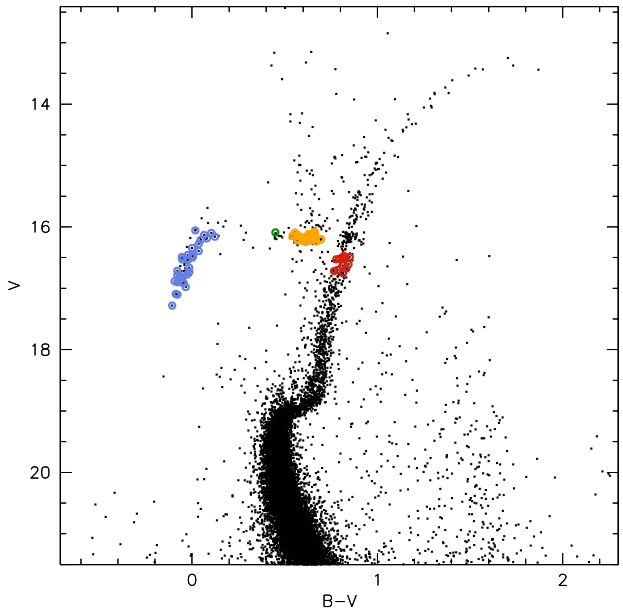

Fig. 2. Colour–magnitude diagram of the inner $1\farcm5 \leq R \leq 10.5$ arcmin region of NGC 1851. Circled stars are those observed in this paper. The colour code is: blue = BHB; green = RR Lyrae variable; orange = RHB; red = RGB.

Figure 2 shows the location of the program stars on the colour magnitude diagram of NGC 1851. Our NGC 1851 ground-based photometric catalogue (see Momany et al. 2004) consists of UBV observations obtained at the Wide-Field Imager (WFI) mounted on the 2.2 m ESO-MPI telescope (La Silla, Chile). Photometric data for the program stars are listed in Table 1. The K magnitudes are from the 2MASS point source catalogue (Skrutskie et al. 2006), and Strömgren photometry is from Calamida et al. (2007).

No information on membership of the program stars to the cluster was available prior to the observations. The very high

Table 1. Basic data for program stars.

Star	RA (J2000)	Dec (J2000)	B (mag)	V (mag)	K (mag)	V_r (km s^{-1})	S/N HR12	S/N HR19
			Blue HB					
3515	5 13 59.619	–39 54 21.26	16.342	16.342	15.688	322.9	26	37
13787	5 13 42.355	–40 09 16.69	16.512	16.538	15.273	316.6	15	30
13858	5 13 44.039	–40 08 48.36	16.312	16.276	15.765	322.6	26	38
20690	5 14 15.237	–40 06 28.88	16.501	16.497	15.742	323.4	17	31
21036	5 14 15.823	–40 06 11.17	16.430	16.394	16.096	320.7	27	35
21285	5 14 21.844	–40 06 00.42	16.723	16.737	15.678	321.3	22	
22551	5 13 59.713	–40 05 20.51	16.864	16.912		320.2	20	26
26345	5 14 12.125	–40 04 11.96	16.196	16.131	15.447	320.9		40
26374	5 14 17.214	–40 04 11.43	16.871	16.917	16.753	314.5	12	27
26686	5 14 01.152	–40 04 07.72	16.461	16.458	15.019	321.4	25	
27792	5 14 02.175	–40 03 53.79	16.945	16.979		330.9		21
27813	5 13 54.243	–40 03 53.69	16.750	16.776	15.131	328.4		25
28043	5 14 09.589	–40 03 50.38	16.433	16.456		319.3		33
28078	5 14 14.805	–40 03 49.81	16.766	16.817		322.0	18	
28346	5 14 05.052	–40 03 46.82	16.267	16.187		322.6	25	44
29743	5 13 57.151	–40 03 30.37	17.025	17.104		324.9		22
31860	5 14 19.417	–40 03 06.26	16.765	16.824		318.2		17
33688	5 13 54.712	–40 02 46.31	16.507	16.526		320.8		32
34973	5 13 55.740	–40 02 32.45	17.005	17.093		326.5	14	
35774	5 14 15.818	–40 02 22.70	16.471	16.468	16.166	321.5		34
35868	5 14 00.891	–40 02 22.26	16.075	16.057	14.014	322.7	35	
36193	5 13 58.666	–40 02 18.30	17.175	17.282		309.2		18
39268	5 14 12.776	–40 01 43.00	16.476	16.529		321.0	21	31
40227	5 14 07.034	–40 01 31.43	16.826	16.902		328.3	16	24
40232	5 14 20.176	–40 01 30.91	16.795	16.859		322.5	18	29
40454	5 14 13.145	–40 01 28.07	16.737	16.801		321.6	17	30
41678	5 14 11.662	–40 01 11.22	16.792	16.886	16.294	321.8	22	
41796	5 14 05.087	–40 01 09.76	16.436	16.491		321.7		30
41951	5 13 58.932	–40 01 07.55	16.258	16.211		329.0		44
43888	5 14 08.812	–40 00 33.76	16.636	16.715	16.590	321.8	23	31
46632	5 14 07.635	–39 59 05.32	16.708	16.787	15.395	320.5	22	
46902	5 14 12.335	–39 58 48.16	16.202	16.098	15.739	315.7	32	39
48007	5 14 03.922	–39 56 57.08	16.284	16.160	15.473	320.1	32	47
52011	5 14 33.081	–40 03 06.99	16.650	16.665	15.861	321.1		27
52576	5 14 53.221	–40 01 53.03	16.767	16.818	15.683	319.8	18	20
			RR Lyrae					
28738	5 13 59.846	–40 03 41.98	16.488	16.122		350		51
			Red HB					
13627	5 13 31.981	–40 10 16.86	16.750	16.120	14.266	318.5	26	51
20785	5 13 56.295	–40 06 23.96	16.859	16.203	14.436	322.0	32	62
21988	5 13 54.295	–40 05 37.13	16.911	16.241	14.381	318.4	36	54
22164	5 13 47.857	–40 05 31.91	16.902	16.210	14.155	319.9	39	62
22393	5 14 07.400	–40 05 24.86	16.851	16.188	14.262	320.9	36	54
22548	5 14 15.569	–40 05 20.03	16.855	16.196	14.258	316.6	40	60
23088	5 14 03.290	–40 05 07.11	16.831	16.169	14.259	318.1	38	65

radial velocity of NGC 1851 (+320.5 ± 0.6 km s^{-1}, Harris 1996) allows to easily rule out field stars: a comparison with the Galactic model by Robin et al. (2003) indicates a probability of ∼2% to find one field interloper among the whole RHB and RGB samples in the same velocity range while the contamination among BHB stars is negligible ($P < 10^{-5}$). So, stars with radial velocities consistent with that of the cluster can be quite safely considered cluster members. On the other hand, all stars observed on the BHB and lower RGB have velocities consistent with that of the cluster, while two of the candidate RHB stars turned out to be disk interlopers. The average radial velocity of the RHB stars is +319.7 ± 0.5 km s^{-1} (rms scatter of 3.7 km s^{-1}), that of BHB stars is +321.6 ± 0.7 km s^{-1} (rms scatter of 4.1 km s^{-1}), and that of the lower RHB stars is +320.3 ± 1.0 km s^{-1} (rms scatter of 3.6 km s^{-1}). All these values agree with the value listed by Harris (1996).

Most of the BHB stars of NGC 1851 are cooler than the Grundahl et al. (1999) u-jump, and could be used in our analysis. Only five stars are warmer than this limit. We did not analyse them because surface abundances for these stars are heavily influenced by the effects of diffusion and radiation pressure, and then results are very difficult to be used in a discussion of original abundances. In addition, while in general we tried to avoid observation of variable stars, star #28738 turned out to be a known RR Lyrae (V12 of Walker 1998), which was shifted out of the instability strip in our photometry. Using data by Walker (1998), we estimated that all our three observations for this star were luckily obtained close to the minimum of the light curve, and could be used for abundance analysis. For this star we then adopted a $B - V = 0.47$, which is the average colour at the observed phases, according to Walker (1998).

Table 1. continued.

Star	RA (J2000)	Dec (J2000)	B (mag)	V (mag)	K (mag)	V_r (km s^{-1})	S/N HR12	S/N HR19
23344	5 14 09.552	–40 05 01.23	16.847	16.211	14.312	319.7		78
24623	5 13 59.896	–40 04 38.47	16.851	16.193	14.273	324.2	38	58
25243	5 14 10.185	–40 04 27.63	16.797	16.149	14.144	322.4	41	61
25336	5 14 16.616	–40 04 26.05	16.812	16.191	14.425	319.8	34	56
25504	5 13 54.500	–40 04 24.52	16.842	16.221	14.291	329.3	35	
25631	5 14 11.546	–40 04 22.25	16.825	16.207	14.325	318.3	33	85
25715	5 13 55.153	–40 04 21.52	16.845	16.182	14.194	320.3		69
25793	5 13 51.233	–40 04 20.51	16.781	16.173	14.383	319.8		78
27604	5 14 04.052	–40 03 56.00	16.849	16.217	14.552	319.0	29	75
28175	5 13 56.135	–40 03 49.23	16.895	16.198	14.195	319.7		72
28746	5 14 01.579	–40 03 41.84	16.828	16.195	14.420	319.7		64
29078	5 14 02.880	–40 03 37.87	16.771	16.111	14.159	317.8	36	
29962	5 14 14.102	–40 03 27.43	16.819	16.181	14.444	317.5	32	
30838	5 14 13.425	–40 03 17.88	16.801	16.179	14.293	321.2		54
31469	5 14 15.520	–40 03 10.78	16.832	16.189	14.317	327.4	36	66
31496	5 13 57.321	–40 03 11.17	16.802	16.188	14.308	333.6	36	
31651	5 13 57.827	–40 03 09.35	16.860	16.210	14.400	319.2		67
31903	5 13 56.378	–40 03 06.35	16.717	16.159	14.477	312.5	36	
32245	5 14 13.430	–40 03 01.87	16.815	16.204	14.461	322.2	34	61
33196	5 14 12.798	–40 02 50.98	16.808	16.185		313.0	38	67
34314	5 14 13.683	–40 02 39.14	16.824	16.183	14.317	321.2	36	68
34386	5 13 54.296	–40 02 38.91	16.746	16.084	14.176	321.6	36	
35789	5 14 14.323	–40 02 22.58	16.756	16.111	14.432	324.1	37	
36599	5 14 27.506	–40 02 12.94	16.822	16.199	14.140	317.6	35	61
37121	5 14 13.327	–40 02 07.68	16.754	16.124	14.372	322.2	34	
37123	5 14 16.085	–40 02 07.57	16.781	16.177	14.358	321.1	34	
38202	5 14 09.724	–40 01 55.85	16.824	16.191	14.321	320.4	41	55
39028	5 13 49.722	–40 01 46.79	16.833	16.229	14.349	318.5		56
39317	5 14 05.012	–40 01 42.74	16.646	16.091	14.119	322.2	33	
39443	5 13 56.321	–40 01 41.54	16.859	16.245	14.338	314.5	39	61
39832	5 13 59.397	–40 01 36.81	16.748	16.118	14.319	317.0	34	
39984	5 13 57.475	–40 01 34.81	16.830	16.215	14.456	325.2	38	63
40117	5 14 03.457	–40 01 32.92	16.815	16.212	14.418	317.4	21	49
40289	5 14 06.028	–40 01 30.55	16.824	16.214	14.466	319.1		64
40450	5 14 02.020	–40 01 28.55	16.790	16.187	14.304	317.4	32	72
40767	5 13 54.626	–40 01 24.45	16.820	16.214	14.313	319.1	34	60
40897	5 14 05.974	–40 01 22.55	16.778	16.183		319.1	40	
41193	5 14 22.824	–40 01 17.83	16.772	16.157	14.308	316.5	39	72
41381	5 14 10.396	–40 01 15.82	16.792	16.222	14.599	313.1	38	
42849	5 14 00.465	–40 00 53.43	16.755	16.169	14.420	316.7	38	
44554	5 14 02.587	–40 00 18.74	16.825	16.227	13.147	317.2	34	64
47239	5 13 55.946	–39 58 23.80	16.832	16.214	14.290	316.5	30	57
47546	5 13 59.563	–39 57 52.78	16.822	16.199	14.442	321.7	33	60
50923	5 14 41.447	–40 05 43.73	16.699	16.129	14.483	319.9	26	61
51490	5 14 36.982	–40 04 16.38	16.829	16.162	14.281	316.2	40	71
51917	5 14 35.031	–40 03 19.04	16.850	16.195	14.524	319.4		56
54362	5 14 42.201	–39 56 59.38	16.687	16.144	14.591	317.3	31	48
			Lower RGB					
20189	5 14 04.735	–40 07 01.94	17.339	16.521	14.398	319.0		56
21830	5 14 06.475	–40 05 41.91	17.344	16.515	14.254	316.5	31	
25497	5 13 59.227	–40 04 24.45	17.452	16.608	14.205	321.8	26	55
25799	5 14 20.707	–40 04 19.53	17.344	16.493	14.226	319.8		56
26532	5 14 11.335	–40 04 09.43	17.293	16.472	14.301	311.9	33	
27085	5 14 08.569	–40 04 02.44	17.306	16.528	14.346	322.3	31	
28445	5 13 56.961	–40 03 45.67	17.567	16.753	14.450	327.2	22	
34604	5 13 50.776	–40 02 36.82	17.487	16.701	14.328	320.6		49
38250	5 14 02.111	–40 01 55.53	17.441	16.628	13.282	323.2	30	
39992	5 14 00.846	–40 01 34.62	17.303	16.490	14.378	321.1		48
45111	5 14 09.575	–40 00 03.16	17.487	16.720	14.324	321.8		45
46657	5 14 10.036	–39 59 03.68	17.316	16.521	14.236	318.5	38	
50876	5 14 35.997	–40 05 53.11	17.512	16.680	14.431	320.7	25	45

Some HB stars rotate with velocities up to a few tens of km s^{-1} (Peterson et al. 1995; Behr et al. 2000a,b; Carney et al. 2008). We checked for fast rotators in our sample examining the *FWHM* of the lines, by cross correlating the spectra with those of templates. No really fast rotator was found in our sample. The only possible moderate rotator is star #27792, for which we obtain a $FWHM = 38.0$ km s^{-1}, with respect to typical values of 27 km s^{-1} for the other BHB stars. This might indicate that this star rotates with $V \sin i \sim 30$ km s^{-1}. However, star #27792 is warmer than 11 500 K and was not included in our abundance analysis.

3. Analysis

3.1. Atmospheric parameters

The analysis follows procedures similar to those adopted in the case of NGC 2808 (Gratton et al. 2011). However, a few modifications were made, so we describe them again.

For the RHB and RGB stars, effective temperatures were derived from the $B - V$, $b - y$, and $V - K$ colours, using the calibration of Alonso et al. (1999; with the erratum of Alonso et al. 2001). The colours were dereddened using the $E(B - V)$ values from the updated on-line version of the Harris (1996) catalogue and the $E(V - K)/E(B - V)$ value from Cardelli et al. (1989). The calibrations require input values for the metallicity [A/H]. We adopted the value obtained by Carretta et al. (2010). We assigned weight 4 to the $B - V$ colours, 5 to the $b - y$, and 1 to the $V - K$ ones, because the program stars are very faint for the 2MASS observations. The comparison between temperatures from $b - y$ and those from the other two indices together yields a mean difference of 0 ± 8 K (rms = 67 K) and 5 ± 20 K (rms = 71 K) for the RHB and RGB stars, respectively. For the RR Lyrae star #28738 = V12, we could only use the $B - V$ value from Walker (1998).

For the blue HB stars, we started from the $(B - V) - T_{\rm eff}$ calibration by Kurucz[5], as in NGC 2808. Infrared colours from 2MASS are not reliable for these faint stars. Furthermore, $B - V$ colours saturate, so that errors in individual temperature values become very large. We then derived effective temperatures from $B - V$ for individual stars ($T_{\rm eff}(B - V)$), but then fitted a quadratic relation between these temperatures and the V magnitudes, and extracted a temperature ($T_{\rm eff}(V)$) entering the V magnitude into this relation. We repeated this procedure using $u - y$ colours from Strömgren photometry rather than V, obtaining a second value for the temperature ($T_{\rm eff}(u - y)$). The adopted $T_{\rm eff}$'s are the average of $T_{\rm eff}(V)$ and $T_{\rm eff}(u - y)$ for individual stars obtained from these relation. Since they are ultimately calibrated against $T_{\rm eff}(B - V)$, these temperatures are on the same scale used for NGC 2808, but they have much smaller internal errors. Note that two stars (#35868 and #46902) are clearly brighter than the mean line for the BHB; they are likely stars evolved off the HB. For these stars, $T_{\rm eff}(V)$ was not considered. On average, $T_{\rm eff}(V) - T_{\rm eff}(u - y) = 33 \pm 52$ K, with an rms of 280 K.

Given these comparisons, we assumed errors of 50, 50, and 200 K as representative values for the internal errors in the temperatures for RHB, RGB, and BHB stars respectively. Systematic errors due to scale errors or incorrect parameters for the cluster are likely larger. We come back later on their potential impact.

The surface gravities were obtained from the masses, luminosities, and effective temperatures. For the masses, we adopted values of 1.00, 0.657, and 0.575 $M_\odot$ for stars on the RGB, RHB, and BHB (see Gratton et al. 2010; and Sect. 4.5 for discussions of values adequate for the different sequences). The bolometric corrections were obtained using calibrations consistent with those used for the effective temperatures (Alonso et al. 1999 for the red giant and RHB stars, and Kurucz for the BHB stars). The adopted distance modulus has been taken from Harris' catalogue.

Errors in gravities are small. The assumption about masses is likely correct within 10%, while those on the effective temperature and luminosity cause errors in gravities not larger than ∼2% for the RHB stars and red giants, and ∼8% for the BHB stars. The error in gravities is then not larger than 0.05 dex for the cool stars and 0.10 dex for the warm ones.

The same metal abundance of [A/H] = –1.2 and microturbulence velocity ξ_μ of 2.0 km s^{-1} were adopted for all RHB stars, and 1.5 km s^{-1} for the RGB ones. The metal abundance is similar to the average value of our Fe abundances for the RHB stars: [Fe/H] = -1.14 ± 0.01 (rms = 0.064 dex). Note that uncertainties in the Fe abundances are much larger than represented by this tiny error bar, which is simply the standard deviation of the mean value. Our average Fe abundance is very close to that derived for RGB stars by Carretta et al. (2010, 2011a: [Fe/H] = –1.16). For the RGB stars we obtained a slightly lower value of [Fe/H] = -1.18 ± 0.03 with a larger rms of 0.11 dex, which is not surprising because on average we measured fewer lines due to smaller spectral coverage and lower S/N of the spectra.

The microturbulence velocity ξ_μ is not well constrained by our data, because the Fe I lines have only a moderate range in equivalent widths. Practically, only the 6065 Å line is saturated enough to really constrain it, so that its value is sensitive to the atomic parameters (oscillator strength and damping constant) we adopted for this line. The gf for this line is from VALD database (Kupka et al. 2000)[6], the damping constant is from Barklem et al. (2000). Taken at face value, the Fe I lines yield a low value for $\xi_\mu = 1.3$ km s^{-1}. On the other hand, some lines of other elements are quite strong. For instance, the Ca I lines at 5857 and 6122 Å are well on the flat part of the curve of growth (see Sect. 3.2 for a discussion of the parameters we adopted for these lines). The adoption of the low value of the microturbulence velocity indicated by the Fe I lines would yield large overabundances of Ca (on average [Ca/Fe] ∼ 0.9), inconsistent with the value derived from giants ([Ca/Fe] = 0.30 ± 0.02: Carretta et al. 2011a,b), which is a typical value for metal-poor stars. The value of ξ_μ we adopted is a compromise, producing only a moderate trend of the Fe abundances with EW and a more acceptable average value of [Ca/Fe] = 0.48. However, these comparisons indicate that our values of the microturbulent velocities have rather large systematic error bars attached, which we estimate at ±0.5 km s^{-1}. We note that the value we adopted is in the middle of the range usually found in previous analysis of BHB stars (Lambert et al. 1992; Behr et al. 1999, 2000b; Kinman et al. 2000; Fabbian et al. 2005; Villanova et al. 2009; Marino et al. 2011).

Two Fe II lines (at 5991.38 and 6084.10 Å) could be measured in RHB spectra and only the first one in RGB ones. Abundances derived from these lines are in fair agreement with those obtained from the Fe I lines: on average we obtained [Fe/H] = -1.20 ± 0.01 and -1.23 ± 0.08 for RHB and RGB stars respectively. This supports the choice of the atmospheric parameters adopted throughout this paper.

Table 2 lists the effective temperatures $T_{\rm eff}$ and surface gravities $\log g$ we used in the analysis of the program stars, as well

[5] See kurucz.harvard.edu

[6] See URL vald.astro.univie.ac.at

Table 2. Atmospheric parameters and Fe abundances.

Star	$T_{\rm eff}$ (K)	log g (dex)	lines	[Fe/H]$_I$ $\langle\rangle$	rms	lines	[Fe/H]$_{II}$ $\langle\rangle$	rms
				Blue HB				
3515	9343	3.35						
13787	10 025	3.50						
13858	9142	3.34						
20690	9981	3.54						
21036	9459	3.44						
21285	10 906	3.76						
22551	11 517	3.83						
26345	8767	3.23						
26374	11 574	3.85						
26686	9721	3.47						
27792	11 986	3.67						
27813	11 083	3.77						
28043	9680	3.42						
28078	11 094	3.72						
28346	8789	3.26						
29743	12 694	3.85						
31860	11 695	3.79						
33688	9976	3.51						
34973	12 562	3.87						
35774	9716	3.48						
35868	9072	3.22						
36193	13 670	4.03						
39268	9980	3.41						
40227	11 368	3.71						
40232	11 316	3.73						
40454	10 957	3.65						
41678	11 762	3.68						
41796	10 006	3.40						
41951	8861	3.27						
43888	10 647	3.50						
46632	10 980	3.59						
46902	8902	3.26						
48007	8751	3.25						
52011	10 730	3.70						
52 576	11 216	3.74						
				RR Lyrae				
28738	6014	2.70	3	–1.22	0.28			
				Red HB				
13627	5441	2.44	16	–1.06	0.13	2	–0.99	0.21
20785	5405	2.46	16	–1.10	0.13	2	–1.06	0.10
21988	5348	2.46	16	–1.17	0.20	2	–1.25	0.05
22164	5306	2.42	16	–1.29	0.22	1	–1.14	
22393	5384	2.45	16	–1.10	0.17	2	–1.14	0.02
22548	5412	2.46	16	–1.14	0.18	2	–1.21	0.06
23088	5369	2.43	16	–1.21	0.14	2	–1.27	0.14
23344	5445	2.48	7	–1.16	0.08			
24623	5415	2.46	16	–1.25	0.16	2	–1.36	0.05
25243	5394	2.44	14	–1.14	0.13	2	–1.24	0.14
25336	5519	2.50	16	–1.07	0.19	2	–1.24	0.23
25504	5411	2.48	9	–1.22	0.18	2	–1.12	0.09
25631	5500	2.50	16	–1.08	0.18	2	–1.16	0.03
25715	5386	2.44	7	–1.22	0.07			
25793	5537	2.50	7	–1.17	0.11			
27604	5471	2.50	16	–1.12	0.18	2	–1.16	0.00
28175	5289	2.41	7	–1.13	0.17			
28746	5424	2.47	7	–1.18	0.13			
29078	5341	2.40	9	–1.13	0.20	2	–1.26	0.06
29962	5464	2.48	9	–1.01	0.14	2	–1.22	0.02
30838	5479	2.48	7	–1.07	0.14			
31469	5417	2.46	16	–1.14	0.22	2	–1.41	0.24
31496	5482	2.49	9	–1.14	0.23	2	–1.17	0.10
31651	5401	2.47	7	–1.15	0.14			
31903	5691	2.55	9	–1.13	0.23			
32245	5497	2.50	16	–1.06	0.20	2	–1.32	0.00

Table 2. continued.

Star	$T_{\rm eff}$	$\log g$		[Fe/H]$_I$			[Fe/H]$_{II}$	
	(K)	(dex)	lines	⟨⟩	rms	lines	⟨⟩	rms
33196	5455	2.48	16	–1.05	0.18	2	–1.12	0.09
34314	5408	2.46	16	–1.10	0.19	2	–1.23	0.08
34386	5339	2.39	9	–1.18	0.06	2	–1.13	0.02
35789	5428	2.44	9	–1.10	0.16	2	–1.29	0.04
36599	5436	2.47	16	–1.13	0.16	2	–1.14	0.05
37121	5452	2.45	9	–1.11	0.17	2	–1.21	0.04
37123	5528	2.50	9	–1.11	0.20	2	–1.30	0.14
38202	5414	2.46	16	–1.20	0.12	2	–1.33	0.16
39028	5477	2.50	7	–1.12	0.12			
39317	5654	2.51	9	–1.04	0.20	2	–1.19	0.10
39443	5456	2.50	15	–1.10	0.12	2	–1.18	0.25
39832	5405	2.43	9	–1.07	0.19	2	–1.28	0.02
39984	5487	2.50	16	–1.07	0.13	2	–0.98	0.08
40117	5472	2.50	15	–1.18	0.26	1	–0.98	
40289	5459	2.49	7	–1.20	0.19			
40450	5483	2.49	15	–1.14	0.16	2	–1.14	0.04
40767	5474	2.50	16	–1.20	0.18	2	–1.31	0.06
40897	5569	2.52	9	–1.11	0.18	2	–1.18	0.02
41193	5477	2.48	16	–1.12	0.18	2	–1.10	0.21
41381	5603	2.55	8	–1.15	0.22	2	–1.14	0.01
42849	5538	2.50	9	–1.22	0.13	2	–1.34	0.09
44554	5520	2.52	15	–1.19	0.13	1	–1.42	
47239	5431	2.48	16	–1.18	0.15	2	–1.25	0.00
47546	5508	2.50	16	–1.13	0.20	2	–1.15	0.01
50923	5653	2.53	14	–1.18	0.25	2	–1.27	0.25
51490	5345	2.42	16	–1.18	0.13	2	–1.14	0.12
51917	5431	2.47	7	–1.36	0.18			
54362	5755	2.57	15	–1.15	0.19	2	–1.31	0.15
				RGB				
20189	4957	2.58	5	–1.35	0.16			
21830	4928	2.56	8	–1.15	0.16	1	–1.55	
25497	4909	2.58	10	–1.13	0.11	1	–1.28	
25799	4932	2.55	7	–1.17	0.15			
26532	4948	2.56	10	–1.09	0.12	1	–1.04	
27085	5015	2.61	10	–1.02	0.13	1	–1.16	
28445	4965	2.67	9	–1.10	0.12			
34604	4983	2.66	7	–1.28	0.19			
38250	4936	2.62	10	–1.09	0.17	1	–1.08	
39992	4937	2.56	5	–1.39	0.14			
45111	5023	2.70	6	–1.24	0.23			
46657	4946	2.58	10	–1.14	0.17	1	–1.13	
50876	4908	2.62	14	–1.25	0.23			

as the abundances for Fe I, Fe II. Table 3 gives the abundances for N I, O I, Na I, Mg I, Mg II, Si I, Ca I, and Ba II. Abundances were estimated from equivalent widths. The analysis is very similar to that described in Gratton et al. (2011) for NGC 2808. In the following section we give details for a few elements, outlining what was changed from that paper.

3.2. Analysis for individual elements

Nitrogen: N abundances were derived only for BHB stars (upper limits were obtained for the cooler stars). They are based on the two high excitation lines at 8216.3 and 8242.4 Å. The first one has been used in the recent analysis of the solar N abundance by Caffau et al. (2009), who obtained a N abundance of $\log n(N) = 7.85$ from this line (for the 1D LTE analysis, which is within 0.01 dex from the value they obtain from the 3-D NLTE one), very close to their recommended value of $\log n(N) = 7.86$. We use the VALD $\log gf$ for this line, which is 0.13 dex lower than the NIST one; with this value, we obtain a solar N abundance of $\log n(N) = 7.99$ using the Kurucz 1D solar spectrum, which is consistent with the difference in the adopted gf's. We conclude that these lines yield abundances consistent with the best estimate of N abundances for the Sun.

On the other hand, non-LTE corrections are likely not negligible for these lines for BHB stars. Statistical equilibrium calculations for N in population I A-type stars have been presented by Przybilla & Butler (2001), who also made comparisons with previous determinations. The stars considered by these authors bracket the surface gravity and line strength range of the stars studied here, though they are more metal-rich. While they do not provide non-LTE corrections for the two lines considered in this analysis, they provide data for many lines of the same lower and close upper levels, which are most likely very close to those appropriate for the lines we could measure. The non-LTE abundance corrections they obtained for these lines are nearly proportional to the EWs, being well reproduced by the same relation Δ[N/Fe] $= -0.0036 \times$ EW for all stars in their sample. We then adopted the corrections given by this relation to the

Table 3. Abundances of other elements.

Star	[N/Fe]	[O/Fe]	[Na/Fe]	[Mg/Fe] I	[Mg/Fe] II	[Al/Fe]	[Si/Fe]	[Ca/Fe]	[Mn/Fe]	[Ba/Fe]
					Blue HB					
3515	1.21	0.24	0.44							
13787	1.19	0.08	0.11		0.68					
13858	1.05	0.12	0.79		0.81					
20690	1.31	–0.50	0.72		0.53					
21036	1.32	0.56	0.45		0.61					
21285			0.31							
22551	1.13	–0.12	<0.81		0.45					
26345	1.12	0.20	0.30		0.72					
26374	1.44	0.02	<0.81		0.71					
26686			<0.02							
27813	1.37	–0.02			0.76					
28043	1.07	0.26			0.62					
28078			1.17							
28346	0.91	–0.10	0.60		0.51					
33688	1.18	–0.04			0.34					
35774	1.15	0.18			0.42					
35868			0.33							
39268	1.18	–0.01	0.69		0.80					
40227	1.23	0.06	1.48		0.52					
40232	1.11	–0.27	<0.76		0.64					
40454	1.25	–0.03	0.73		0.07					
41796	1.10	–0.37								
41951	1.12	0.15			0.55					
43888	1.04	–0.12	<0.56		0.58					
46632			0.56							
46902		–1.20	–0.56							
48007	0.81	0.31	0.99		0.12					
52011	1.31	0.37			1.10					
52576			<0.71							
					RR Lyrae					
28738	1.03	0.17	0.51	<–0.34						
					Red HB					
13627		0.26	–0.07	0.41			0.16	0.64		0.23
20785		0.37	–0.10	0.41			0.16	0.45		0.16
21988		0.15	–0.17	0.34		0.12	0.23	0.20		0.22
22164		0.27	–0.10	0.25			0.18	0.20		0.13
22393		0.16	–0.20	0.35			0.30	0.30		–0.17
22548		0.39	–0.07	0.24			0.21	0.17		–0.10
23088		0.46	–0.21	0.40		–0.16	0.19	0.16		–0.02

abundances we derived from the LTE analysis. The corrections are quite uniform, with a mean value of –0.28 dex. Although it is clear that this is a rough procedure that may bring some additional uncertainty, we deem unlikely that these corrections are in error by more than half this value. After this correction, the N abundances are very uniform among the BHB stars, with an average value of [N/Fe] = 1.16 ± 0.15. The error bar is here the rms scatter of individual values and agrees with internal errors. We plotted these N abundances against various quantities (including O and Na abundances); we only found a small trend for increasing N abundances with effective temperature, with stars with $T_{\rm eff}$ < 9000 K having N abundances some 0.1–0.2 dex below the average, and those with $T_{\rm eff}$ > 11 000 K with N abundances higher than average by a similar amount. This small trend might either be real (warmer stars on the HB might indeed be expected to be more N-rich), or an artifact of the analysis, since the trend is at the level where we expect possible systematic errors.

We looked for the N lines in the spectra of the RHB stars. The line at 8216.3 Å is in a difficult region, with strong telluric lines that must be subtracted with care. We looked for but did not detect the 8242.6 Å line in the summed spectrum of the RHB stars; we may set an upper limit of EW < 3 mÅ, which yields [N/Fe] < 1.1. We also looked for this line in individual spectra but we did not detect it in any. For instance, the robust upper limit of 15 mÅ we get for the warm, Ba-rich star #54362 implies [N/Fe] < 1.55, which is distinctly lower than the value for the most N-rich bright red giant observed by Yong et al. (2009). In order for this upper limit to coincide with such a high N abundance, our temperature scale for RHB should be lowered by 200 K, which we deem quite unlikely.

Oxygen: Oxygen abundances have fairly large errors, especially for BHB stars. This is because, due to the geocentric radial velocity of NGC 1851 stars, the telluric emission line at 7780.4 Å (Hanuschik 2003) falls very close to the strongest line of the triplet. This makes the sky subtraction uncertain for the faintest stars (the BHB ones) in our sample. As in the case of NGC 2808, we applied the non-LTE corrections by Gratton et al. (1999) for RHB and RGB stars and the RR Lyrae variable, and from Takeda (1997) for BHB stars.

Table 3. continued.

Star	[N/Fe]	[O/Fe]	[Na/Fe]	[Mg/Fe] I	[Mg/Fe] II	[Al/Fe]	[Si/Fe]	[Ca/Fe]	[Mn/Fe]	[Ba/Fe]
23344		0.36	0.03	0.38			0.09			
24623		0.46	–0.08	0.36			0.04	0.25		–0.13
25243		0.38	–0.03	0.38			0.25	0.44		0.12
25336		0.29	–0.01	0.51			0.01	0.51		0.01
25504			–0.17				0.10	0.55		0.32
25631		0.14	0.16	0.48			0.24	0.37		0.68
25715		0.37	–0.17	0.31			0.09			
25793		0.39	0.46	0.43		0.07	0.23			
27604		0.31	0.08	0.42			0.26	0.71		0.22
28175		0.47	0.03	0.39			0.25			
28746		0.39	–0.18				0.13			
29078			0.10				0.14	0.52		0.29
29962			–0.03				0.07	0.40		0.38
30838		0.19	0.51	0.43			0.16			
31469		0.26	0.01	0.32			0.26	0.51		0.34
31496			0.06				0.23	0.28		0.05
31651		0.34	–0.09	0.43			0.19			
31903			0.93				0.23	0.64		1.19
32245		0.54	0.07	0.37			0.18	0.25		0.25
33196		0.31	0.00	0.40			0.21	0.26		0.13
34314		0.47	–0.04	0.40			0.11	0.55		0.26
34386			0.02				0.32	0.39		0.08
35789			–0.10				0.25	0.42		0.34
36599		0.33	0.04	0.43			0.21	0.30		0.13
37121			0.40				0.39	0.52		1.18
37123			0.42				0.39	0.32		1.19
38202		0.07	–0.15	0.38			0.07	0.52		–0.08
39028		0.25	–0.04	0.42			0.19			
39317			0.44				0.37	0.47		0.01
39443		0.30	–0.04	0.47			0.19	0.44		0.28
39832			0.04				0.22	0.62		0.15
39984		0.32	0.11	0.33			0.27	0.38		0.34
40117		0.32	0.21	0.49			0.22	0.64		–0.02
40289		0.28	0.03	0.42			0.12			
40450		0.46	–0.17	0.43			0.28	0.42		0.22
40767		0.17	–0.11	0.31			0.11	0.50		0.03
40897			–0.01				0.25	0.51		0.17
41193		0.37	–0.08	0.45			0.00	0.37		0.06
41381			0.25				0.13	0.54		1.10
42849			0.20				0.30	0.23		0.26
44554		0.31	0.14	0.34			0.16	0.22		0.63
47239		0.38	–0.13	0.38			0.31	0.42		0.06
47546		0.32	0.51	0.48			0.12	0.51		1.10
50923		0.12	0.48	0.36			0.01	0.60		–0.36
51490		0.35	–0.20	0.37			0.29	0.24		–0.10
51917		0.25	–0.23	0.35			0.04			
54362	<1.55	0.00	0.43	0.48			0.28	0.46		0.93
					RGB					
20189		0.48	0.06	0.31			0.12			
21830			0.12				0.33	0.26	–0.47	0.02
25497			0.02				0.07	0.22	–0.50	0.02
25799		0.72	–0.19	0.27			–0.07			
26532			0.25				0.44	0.26	–0.41	0.73
27085			0.16				0.24	0.21	–0.26	0.80
28445			0.02				0.38	0.33	–0.36	1.24
34604		0.50	0.05	0.42			0.18			
38250			–0.19				0.29	0.27	–0.36	0.48
39992		0.22	–0.02	0.39			0.10			
45111			–0.11	0.33			0.21			
46657			–0.25				0.08	0.15	–0.46	0.01
50876		0.30	0.05	0.43			0.04	–0.01	–0.64	0.69

Sodium: In all spectra the D1 line is blended with the interstellar D2 line, and cannot be measured accurately[7]. In addition, we could use the doublet at 8183–94 Å in all RHB and RGB stars, and in cooler BHB ones.

For RHB stars we adopted the non-LTE corrections by Gratton et al. (1999). For the stars of interest here they are typically negative and small in absolute value: ∼−0.15 and ∼−0.05 dex for the D2 line and the 8183–94 Å doublet respectively. Had we applied the updated corrections by Lind et al. (2011), these would have been much larger in absolute value (∼−0.55 and ∼−0.40 dex, respectively). However, we prefer to keep the older values by Gratton et al. (1999) for uniformity with the analysis of red giants by Carretta et al. (2009) and of the stars in NGC 2808 (Gratton et al. 2011). This comparison shows that quite large offsets can be present in our Na abundances, although the star-to-star values are almost unaffected by this uncertainty.

For the BHB stars we used the non-LTE corrections by Mashonkina et al. (2000), as done for the BHB stars in NGC 2808. A discussion of the impact of these non-LTE corrections can be found in Gratton et al. (2011).

On average, the D2 lines give higher Na abundances than the doublet at 8183–94 Å: RHB: $[Na/Fe]_{D2} - [Na/Fe]_{IR} = 0.13 \pm 0.03$ dex (30 stars, rms = 0.16 dex); RGB: $[Na/Fe]_{D2} - [Na/Fe]_{IR} = -0.35$ dex (1 star); BHB: $[Na/Fe]_{D2} - [Na/Fe]_{IR} = 0.45 \pm 0.15$ dex (3 stars, rms = 0.27 dex). This difference may be attributed to the not perfect LTE corrections.

Magnesium: Mg abundances for RHB and RGB stars are based on the Mg I line at 8213.04 (Gratton et al. 2011) and those for BHB on the Mg II lines at 7877.06 and 7896.38 Å. For RHB and RGB stars we obtain a very small star-to-star scatter (only 0.06 dex), fully consistent with a single Mg abundance of $[Mg/Fe] = 0.39 \pm 0.06$. The abundance scatter is much larger for BHB stars (0.23 dex). This may be interpreted either as a real result (a Mg-Na anticorrelation) or as analysis scatter.

Aluminium: The high excitation doublet at 7835.3–36.1 Å was not detected in our spectra for individual stars, either on the RGB or RHB. This sets an upper limit of $[Al/Fe] < 0.2$. The Al feature is not even unambiguously detected in the sum of all the RHB spectra: in this case we detected a very weak feature which might possibly be identified with the strongest component of the doublet (the 7836.1 Å line) with $EW = 1.7$ mÅ, which yields $[Al/Fe] \sim -0.6$.

Calcium: We derived LTE Ca abundances for RHB and RGB stars from the 5857 and 6122 Å lines. Accurate oscillator strengths are available for these lines from VALD; we adopted the same damping constants used by Mashonkina et al. (2007). Non-LTE corrections are expected to be small (see Mashonkina et al. 2007). Since the lines are quite strong, they are quite sensitive to the adopted value for the microturbulent velocity. As mentioned in Sect. 3.1, our Ca abundances for RHB stars are quite high.

Barium: The Ba abundances are based on the Ba II line at 5853.69 Å, which is quite strong in the spectra of RHB and RGB stars (this line is not expected to be detectable in BHB stars). The line parameters adopted in our analysis are the same of Mashonkina & Zhao (2006), including the collisional damping constant. Note that hyperfine structure should be negligible for this line (total width <8 mÅ). We are not aware of statistical equilibrium computations for Ba appropriate for this line and for model atmosphere parameters in the range of the program stars. However, departures from LTE are not expected to be very large (see Korotin et al. 2011).

[7] There are large star-to-star variations in the strength of the interstellar D1 line. Large EWs were obtained for stars located along two filaments, running approximately E-W and located north and south respectively of the cluster center. These large variations make it impossible to use e.g. the warmest HB stars to subtract the interstellar D2 component from the blend with the stellar D1 line.

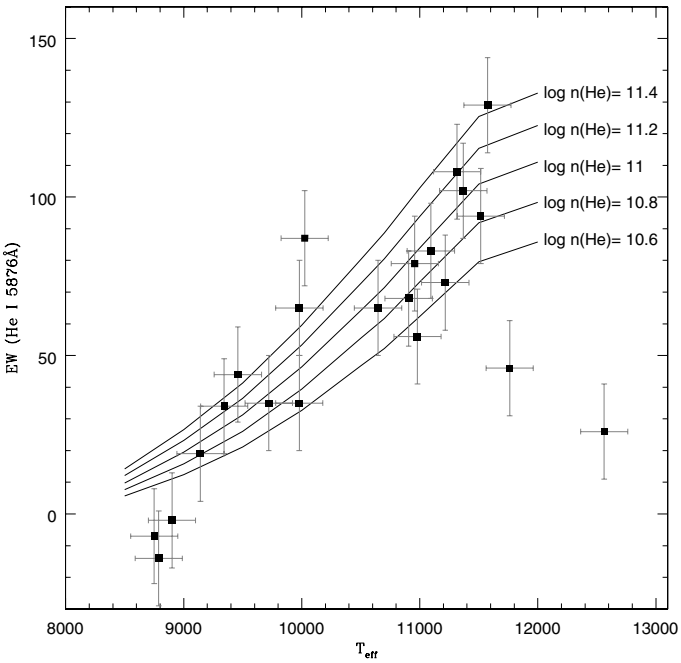

Fig. 3. Run of the EW of the He I line at 5876 Å as a function of $T_{\rm eff}$ along the BHB of NGC 1851. Overimposed are lines of constant He abundance ($\log n$(He) = 10.6, 10.8, 11.0, 11.2 and 11.4). These curves have been computed for gravities appropriate to the location along the BHB.

3.3. He abundances

He abundances were obtained using the narrow multiplet at 5875.6 Å. Figure 3 compares the run of the EWs for this line with that expected for model atmospheres of different temperatures, computed with parameters appropriate for the HB of NGC 1851, and different values of the He abundances. The points relative to individual stars display a rather large scatter, mainly due to errors in the EWs, which are quite large given the fairly low S/N of the spectra. This rather large scatter precludes the use of the He abundances to discuss properties of individual stars. However, the rather large number of stars available allows to derive a sensible average value of $\log n$(He) = 11.01 ± 0.10, which corresponds to an abundance in mass of $Y = 0.291 \pm 0.055$. While the error bar of this average value is still quite large, it agrees fairly well with expectations for a population with an initial He abundance as given by the Big Bang alone ($Y = 0.248$: Cyburt 2004) and later modified by the effect of the first dredge-up, which is $\Delta Y \sim 0.015$ for the stars under consideration (Sweigart 1987). The error bar is large enough to accommodate a moderate He enhancement; however very large initial He abundances ($Y > 0.33$) are not compatible with the present result. This agrees with the lack of evidence for a broadening of the main sequence (Milone et al. 2008). A normal helium was also found using the R-parameter (Salaris et al. 2004).

Table 4. Sensitivity and error analysis.

Parameter	$T_{\rm eff}$	log g	[A/H]	$v_{\rm t}$	EW	Total
Variation	+100 K	+0.5 dex	+0.1 dex	+0.5 km s^{-1}	+10 mÅ	
Error BHB	200 K	0.1 dex	0.05 dex	0.5 km s^{-1}	13 mÅ	
Error RHB	50 K	0.05 dex	0.05 dex	0.5 km s^{-1}	8 mÅ	
Error RGB	50 K	0.05 dex	0.05 dex	0.5 km s^{-1}	8 mÅ	
			Blue HB			
[N/Fe]	0.018	0.049	–0.001	–0.057	0.092	0.138
[O/Fe]	0.021	–0.002	–0.012	–0.154	0.099	0.205
[Na/Fe]	0.087	–0.169	0.000	–0.057	0.162	0.281
[Mg/Fe]	0.000	0.052	–0.004	–0.056	0.144	0.196
			Red HB			
[Fe/H]	0.065	–0.020	–0.001	–0.098	0.050	0.078
[O/Fe]	–0.095	–0.181	0.000	–0.081	0.080	0.095
[Na/Fe]	0.095	–0.125	0.003	–0.126	0.049	0.098
[Mg/Fe]	0.025	–0.015	0.000	–0.022	0.160	0.129
[Si/Fe]	0.030	0.005	0.001	–0.027	0.094	0.078
[Ca/Fe]	0.075	–0.100	0.000	–0.200	0.158	0.155
[Ba/Fe]	0.056	0.181	0.006	–0.169	0.181	0.180

Notes. Variation is the change in each parameter used in the sensitivity analysis (Cols. 2–6), while error is the change used to estimate the total error (Col. 7).

3.4. Error analysis

Error analysis was done in the usual way, by repeating the abundance derivation by modifying a single parameter each time. Relevant data are given in Table 4. The last column gives an estimate of the total internal errors obtained using the sensitivities listed above, as well as the errors in the individual parameters given on lines 2 and 3 for blue and red HB stars, respectively.

4. Discussion

4.1. The Na-O anticorrelation

Figure 4 shows the Na-O anticorrelation we obtain for the HB stars of NGC 1851. Different symbols are used for blue and red HB stars. For comparison, we also plotted the Na-O anticorrelation for red giants by Carretta et al. (2011). We remind that the HB stars hotter than 11 500 K are not considered here because their surface abundances are not related in a simple way to their original composition. However, only ∼5% of the HB stars of NGC 1851 are that warm.

On the whole, we obtain a clean Na-O anticorrelation with an inter-quartile of IQR(Na/O) = 0.70 ± 0.41, which is very similar to the value obtained for the RGB by Carretta et al. (2011: IQR(Na/O) = 0.69). On the other hand, the relation between O and Na abundances with colour/temperature is not as clear as it was the case for NGC 2808 and there is considerable overlap between the range of O and Na abundances covered by BHB and RHB stars (see Fig. 5).

More in detail, we compare in Fig. 6 the distribution in [Na/Fe] of BHB and RHB stars. For comparison the same distribution using the abundances of RGB stars by Carretta et al. (2011b) are also shown. It is apparent that RHB stars distribute in two well defined groups: a "majority" group (including 36 stars) have [Na/Fe] < 0.3 and a small group (5 stars) have [Na/Fe] > 0.3. The statistics is improved by considering also the stars that have not been observed with HR19, and then have no O abundance. The subdivision in two groups is still very clean after this addition: there are in total 46 Na-poor and 8 Na-rich stars. In addition, one star (#31903) has a very high [Na/Fe] = 0.93.

The RR Lyrae variable has Na and O abundances very close to that found for the group of Na-rich and moderately O-poor RHB stars.

The BHB stars also define a Na-O anticorrelation, including both O-rich ([O/Fe] ∼ 0.3) stars with moderate Na excesses ([Na/Fe] ∼ 0.5) and a prominent group of O-poor ([O/Fe] ∼ 0.2) and Na-rich ([Na/Fe] ∼ 0.7) stars. However, the large errors associated to individual BHB stars do not allow to understand if the distribution is continuous or bimodal: this ambiguity is even more evident if we consider also the stars for which no information about the O abundance was available, which spread over a large range of Na abundances (see Fig. 6). There are even two stars (#28078 and #40227) for which we get [Na/Fe] > 1.

On the whole, we obtain a correlation between the [Na/O] abundance ratio and colour of the stars (see Fig. 5). However, while this correlation is very clean for the RHB stars (the Spearman ranking test gives a probability smaller than 0.05% that the observed correlation is random), it is much less clear within the BHB ones (in this case the probability is only smaller than 7%), although on average they have lower O and higher Na abundances (for the whole sample, the probability of a random result is smaller than 0.05%; see Fig. 5). To further complicate the interpretation of observational data, we must take into account the possibility of systematic offsets between the abundances obtained for RHB and BHB stars, mainly related to uncertainties in the non-LTE correction. This result of our analysis should then be taken with some caution, and it is well possible that there is no real offset in Na abundances between RHB and BHB stars. However, we deem the conclusion that O-Na anticorrelations do exist separately for both BHB and RHB stars robust.

4.2. CNO in BHB stars

Cassisi et al. (2008) and Ventura et al. (2009) suggested that the f-SGB is due to a CNO rich population that is also responsible for the BHB. We may compare the prediction of this hypothesis (the BHB are CNO-rich) with our results. We obtain average values of [N/Fe] = +1.16 and [O/Fe] = 0.00 for the

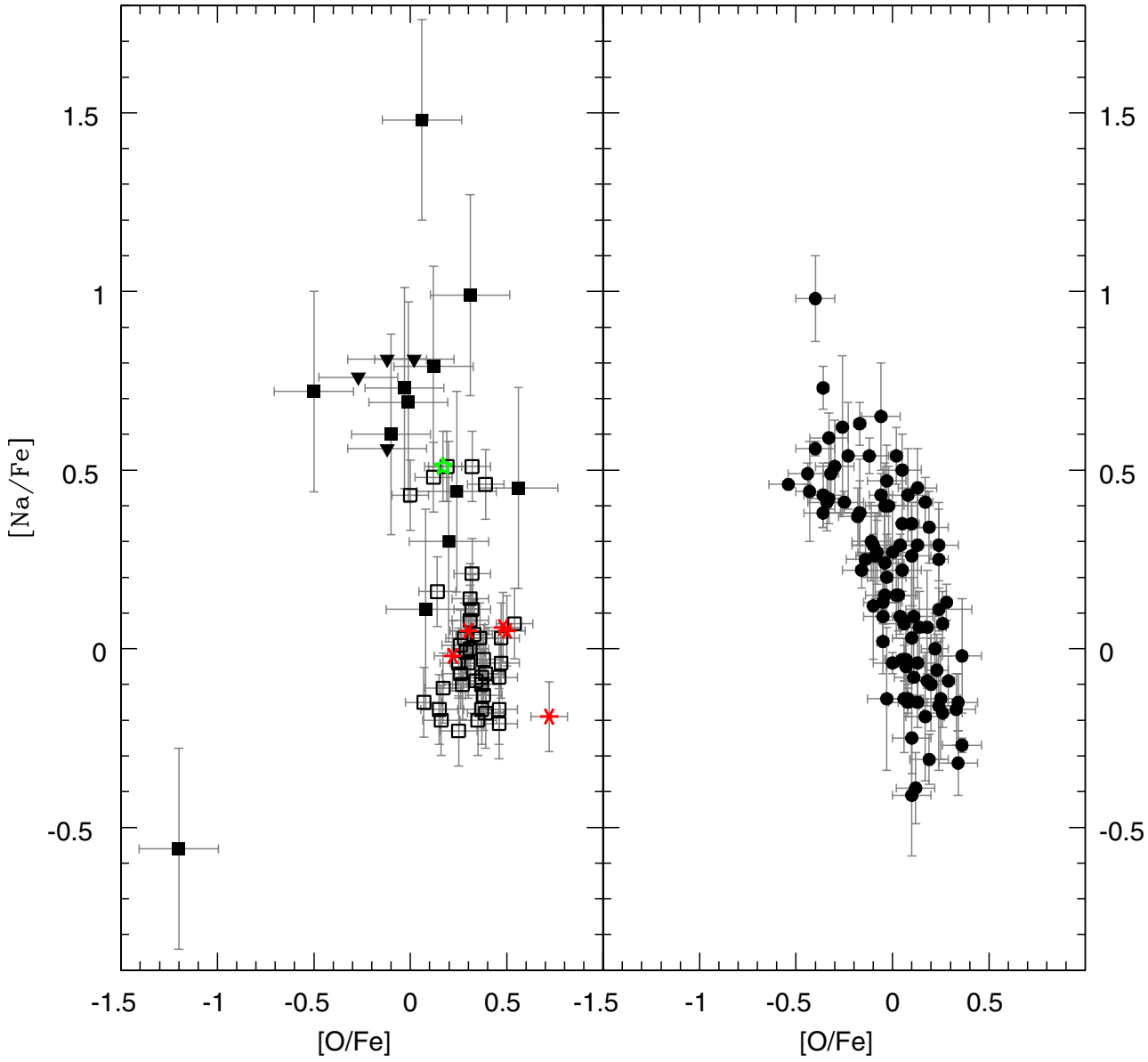

Fig. 4. *Left panel*: Na-O anticorrelation for HB stars of NGC 1851. Filled squares are BHB stars (filled triangles are upper limits for Na); the open star is the RR Lyrae variable; open squares are RHB stars; the asterisks are red giants. *Right panel*: the same distribution for RGB stars from Carretta et al. (2011b).

BHB stars. We have not determined the C abundances. However, both Yong et al. (2009) and Villanova et al. (2010) have obtained C abundances for several stars on the RGB, and did not find any stars with [C/Fe] > −0.2; the average values are [C/Fe] ∼ −0.7 in both studies, with little dispersion. If we then assume that C gives a negligible contribution to the total CNO abundance in the BHB stars of NGC 1851, we find a total of [(C + N + O)/Fe] ∼ 0.24, a value which is fairly typical for metal-poor stars. Since we get a lower limit of [(C+N+O)/Fe] > 0.12 simply considering the O abundance of the Na-poor stars, we conclude that there is no evidence for a significant (Δ[(C+N+O)/Fe] > 0.2) excess of CNO elements among BHB stars in NGC 1851, at variance with the prediction of the Cassisi et al. and Ventura et al. scenario.

4.3. Ba and N abundances in RHB stars and their relation with Na abundances

The Ba abundances also provide useful information in NGC 1851. Yong et al. (2008, 2009), Villanova et al. (2010), and Carretta et al. (2011a) have obtained clear correlations between Na and Ba abundances and have shown that the large Ba abundances found in several RGB stars of NGC 1851 can be attributed to the *s*-process. This suggests an important contribution by thermal pulsing AGB stars to the chemical evolution of this GC. Here, we measured Ba abundances for 44 RHB and eight RGB stars but we have no information about Ba in the BHB stars and the RR Lyrae variable. We obtain a clear correlation between Na and Ba abundances (see Fig. 7). A small part of this correlation might be explained by scatter in the appropriate value for the microturbulent velocity for individual stars, since these lines are quite strong and we adopted the same value for this parameter in all stars. However, the correlation extends over a very broad range and extreme values cannot be explained in this way.

We recall that Carretta et al. (2011a) found a large spread in Ba abundances along the RGB. Ten stars in their sample (9±3%) are clearly Ba-rich ([Ba/Fe] > 0.7), while the remaining ones distribute over the range 0.1 < [Ba/Fe] < 0.7. This latter

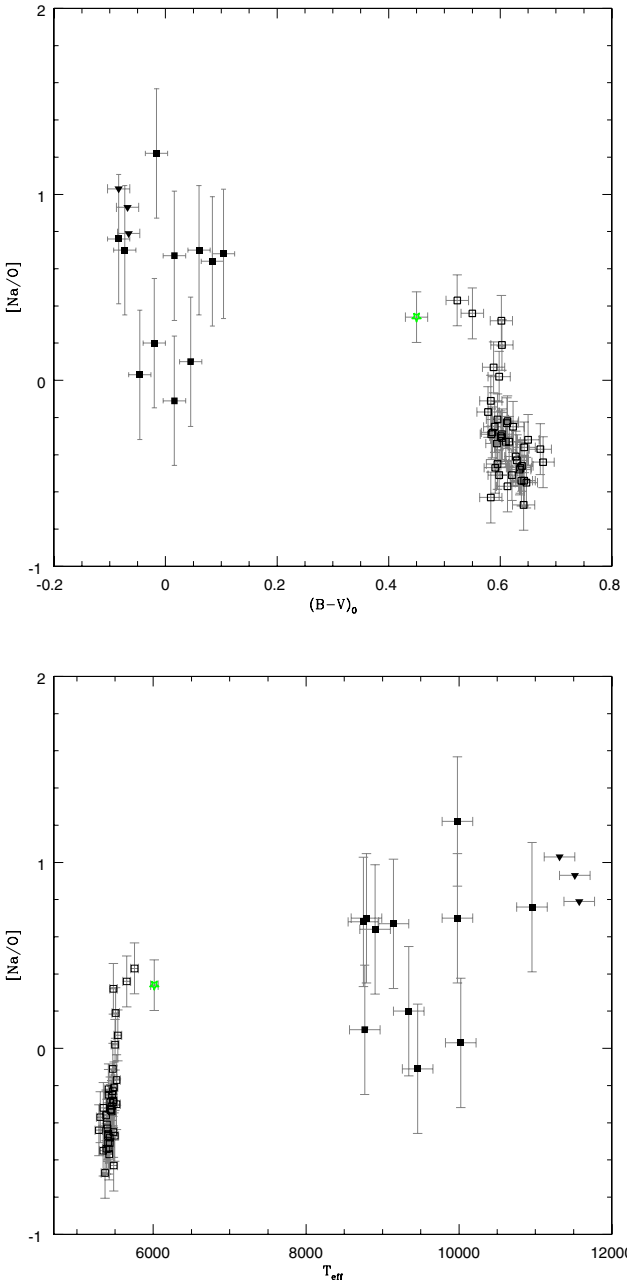

Fig. 5. *Upper panel*: run of the [Na/O] abundance ratio with $B-V$ colour along the HB of NGC 1851 (*left panel*). *Lower panel*: the same, but with $T_{\rm eff}$. Symbols are the same as in Fig. 4.

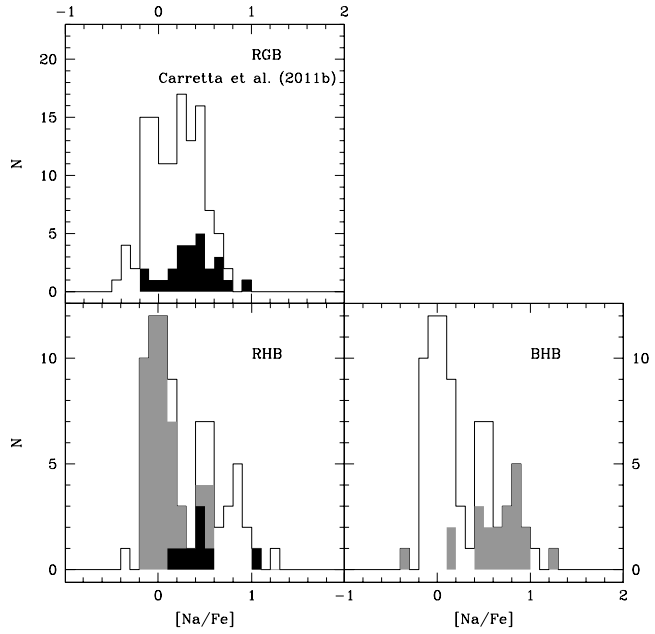

Fig. 6. Distribution of [Na/Fe] abundances for the HB stars analyzed in this paper (*bottom panels*) and for the RGB stars of Carretta et al. (2011b) (*upper panel*). Grey histograms indicate the distribution of RHB (*bottom-left panel*) and BHB (bottom-right panel) stars. Black histograms indicate the distribution of stars with [Ba/Fe] > 0.6.

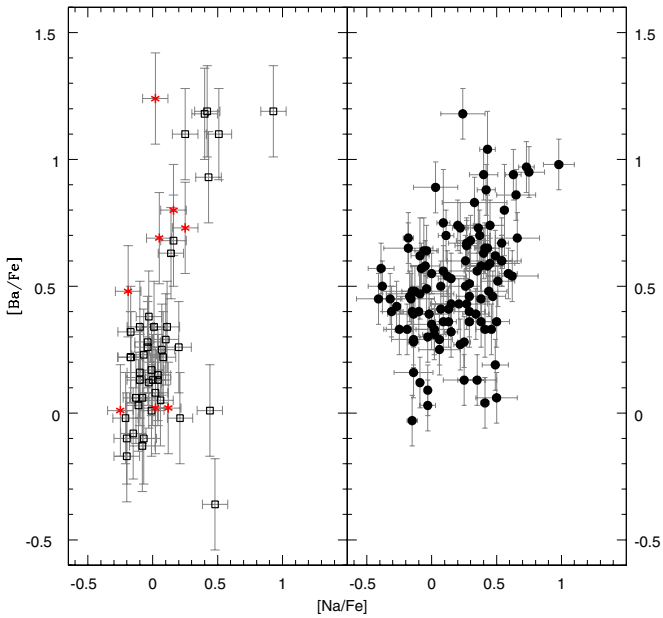

Fig. 7. Correlation of the [Na/Fe] and [Ba/Fe] abundance ratios for stars of NGC 1851. *Left panel*: HB stars; *right panel*: RGB stars from Carretta et al. (2011b). Symbols are the same as in Fig. 4.

scatter might be related to the use of a not optimal line (the 6141 Å one, which is blended with a Fe I line). However, in that work the group of Ba-rich stars tends to have on average larger abundances of Na (0.2 < [Na/Fe] < 0.5; see Fig. 6). On the other hand, our RHB stars clearly divide into two groups: seven stars are Ba-rich ([Ba/Fe] > 0.7), the remaining are Ba-poor ([Ba/Fe] < 0.4). Since RHB makes up ∼60% of the HB stars in NGC 1851, Ba-rich RHB stars should be ∼10 ± 4% of the stars, while Ba-poor correspond to ∼50 ± 4%. The identification of Ba-rich RHB and RGB stars is quite obvious. For exclusion, we then suggest that the BHB stars (for which we did not measure Ba abundances) join the remaining RHB stars being Ba-poor.

We notice that the fraction of Na/Ba-rich RGB stars is consistent with the fraction of stars along the anomalous $v-y$ sequence (∼7%: see Carretta et al. 2011b). Indeed all stars on the anomalous red RGB in the v, $(v-y)$ diagram are Ba-rich (Villanova et al. 2010; Carretta et al. 2011a). The Strömgren colours of this sequence indicate very strong CN bands, which

might be explained either by an extremely large N abundance[8], or by a C abundance comparable to that of O in the atmospheres of these stars, leaving a lot of C available for the formation of C-bearing molecules such as CN and CH in cool RGB stars (see Carretta et al. 2011b). In the second case, since Ba-rich stars are Na-rich and moderately O-poor, C abundances do not need to be extraordinary large, and even a moderate excess of C+N+O might explain observations. The direct determination of the CNO content for a few stars of this sequence by Yong et al. (2011) indicates a low C ([C/Fe] ∼ −0.7) and a very high N content (up to [N/Fe] ∼ +2.2), favouring the first explanation, since they find [(C+N+O)/Fe] ≥ 1.0 for the most extreme stars. The same Yong et al. (2011) caution however that use of NH rather than CN (the specie considered for the NGC 1851 analysis) provide fairly lower N abundances (up to 0.44 dex) for RGB stars in NGC 6752. Were this same difference be valid for NGC 1851, a less spectacular but still quite high [(C+N+O)/Fe] ∼ 0.6 would be obtained for the same stars. Villanova et al. (2009) only published the sum of the CNO abundances (which they found to be [(C + N + O)/Fe] ∼ 0.2 for both the Ba-rich and Ba-poor stars), but they kindly provided us with the values they obtained for the individual elements. They also found low C abundances in all the stars they examined, the mean value for the stars on the Ba-rich sequence being [C/Fe] = –0.58. For the same stars they also found [N/Fe] = 1.09 and [O/Fe] = –0.15. For stars in the Ba-poor sequence they obtain [C/Fe] = –0.88, [N/Fe] = 0.71 and [O/Fe] = 0.09. While C and O abundances agree fairly well with those of Yong et al., the N abundances are very different, which is surprising since the same CN lines are used in both analyses. We conclude that the exact values of the CNO abundances in the RGB Ba-rich stars is still uncertain, although they are definitely more N-rich and C- and O-poor than the RGB Ba-poor stars.

We have not measured the sum of C+N+O for the RHB stars. However, the lack of detection of the N I line at 8216 Å yields an upper limit to the N abundance of [N/Fe] < 1.55 for the warm Ba-rich star #54362, which has [O/Fe]=0.00. Given the possible systematic errors in N abundances from CN lines and the error bar of our determination, this is perhaps not incompatible with the results of Yong et al. for Ba-rich RGB stars, and agrees with that of Villanova et al. If we now assume that the C contribution to the sum of C+N+O is negligible, as found for stars along the RGB, we get an upper limit of [(C+N+O)/Fe] < 0.5 for this star. Taken literally, the comparison between the upper limit for the Ba-rich RHB star and the BHB ones indicates an excess of C+N+O smaller than a factor of 2 for the first star. This is lower than the range in CNO abundances estimated by Yong et al., and in agreement with that by Villanova et al. On the other hand, assuming [(C+N+O)/Fe] ∼ 0.15 is however enough to explain the anomalous $v - y$ colours of these stars. There are several possible sources of errors in this determination, including systematic errors in the atmospheric parameters or departures of real atmospheres from the model ones. Also, it is possible that star #54362 is not a typical Ba-rich star (the Ba excess of [Ba/Fe] = +0.93 is lower than that obtained for a few other stars). However, this comparison suggests that after all the Ba-rich RHB stars might possibly be not particularly rich in the sum of C+N+O.

[8] We estimated the impact of a very large N abundance on $v - y$ computing synthetic Strömgren colours for for a red giant with the same approach of Carretta et al. (2011b). We considered the case of a red giant with M_V = −1, [Fe/H] = –1.3, [C/Fe] = –0.6, [N/Fe] = 1.7, and [O/Fe] = –0.1, and compared its $v - y$ colour with those obtained for a more normal composition ([C/Fe] = –0.6, [N/Fe] = 1.4, and [O/Fe] = –0.1). We found that an extremely N-rich star has a $v - y$ colour 0.41 mag redder than the "normal N-rich" one. This comparison shows that the anomalous $v - y$ sequence can be produced by [N/Fe] ∼ 1.55, which implies a CNO excess of only ∼0.15 dex with respect to normal stars in NGC 1851.

4.4. The Na/Ba poor and Na/Ba-rich RHB stars in the colour-magnitude diagram

The Na-poor RHB stars have a very small range in $B - V$ and Strömgren colours, and hence $T_{\rm eff}$ (∼200 K peak-to-valley). They appear as a very compact group in all diagrams we plotted. The Ba-rich RHB stars are bluer (by 0.044 ± 0.012 mag in $B - V$), warmer (by 148 ± 32 K), and on average slightly brighter than the other RHB stars: the difference in V magnitude is small (−0.035 ± 0.012 mag) but significant at almost 3−σ. The two groups of RHB stars separate clearly in the colour-magnitude diagram, because differences of average values are larger than the internal scatter of each group.

The luminosity difference between Ba-rich and Ba-poor RHB stars might in principle be explained in various ways. For instance, it might be attributed to a difference of $\Delta Y \sim 0.008$ in the He content. However, a difference in He abundance alone would not explain why the RGB Ba-rich stars (likely the progenitors of the RHB Ba-rich stars) have anomalous $v - y$ colours. This hypothesis is then not enough to justify all observations.

A difference in HB luminosity similar to that observed would also be produced by a change of 0.1 dex in metallicity, were the Na-rich more metal-poor than the Na-poor ones. However Na-rich RHB stars have [Fe/H] = −1.121 ± 0.015, rms = 0.045 dex, and Na-poor ones [Fe/H] = −1.147 ± 0.010, rms = 0.066 dex. This is not likely to produce appreciable differences in both luminosity and colours. Therefore this hypothesis does not agree with observations.

Furthermore, since CNO abundance variations have been widely proposed to explain the SGB and HB of NGC 1851 (Salaris et al. 2008; Cassisi et al. 2008; Ventura et al. 2009), it is useful to consider if they can justify these observations. However, while CNO-rich HBs are indeed brighter than CNO-normal ones, they are expected to be also much redder (Lee et al. 1994; Pietrinferni et al. 2009), while they are bluer. This solution is then not acceptable too.

We finally note that there are two Na-rich and Ba-poor RHB stars (#39317 and #50923). They are ∼300 K warmer and ∼0.1 mag brighter than the average RHB stars. We suggest that these two stars evolved well off their ZAHB locations, which were possibly on the BHB or within the instability strip. Incidentally, the only RR Lyrae variable is Na-rich, but unluckily we do not have Ba abundance determination for this star.

4.5. Comparison with simulated HBs

To look for an explanation of the conundrum of the Ba-rich RHB stars, we have to consider differences in more than a single parameter between Ba-rich and Ba-poor RHB stars. For instance, we may assume that the Ba-rich stars are not only more rich in CNO elements (which may explain the anomalous $v - y$ colour on the RGB), but also older (and then less massive) than the Ba-poor RHB stars. In the scenario where the separation between BHB/f-SGB and RHB/b-SGB sequences is due to an age difference of about 1 Gyr, this corresponds to attributing to the Ba-rich stars an age more similar to the first group or at least intermediate between the two. To explore this possibility, we ran some simulation for the HB of NGC 1851. They were performed as described in Salaris et al. (2008) and we adopted

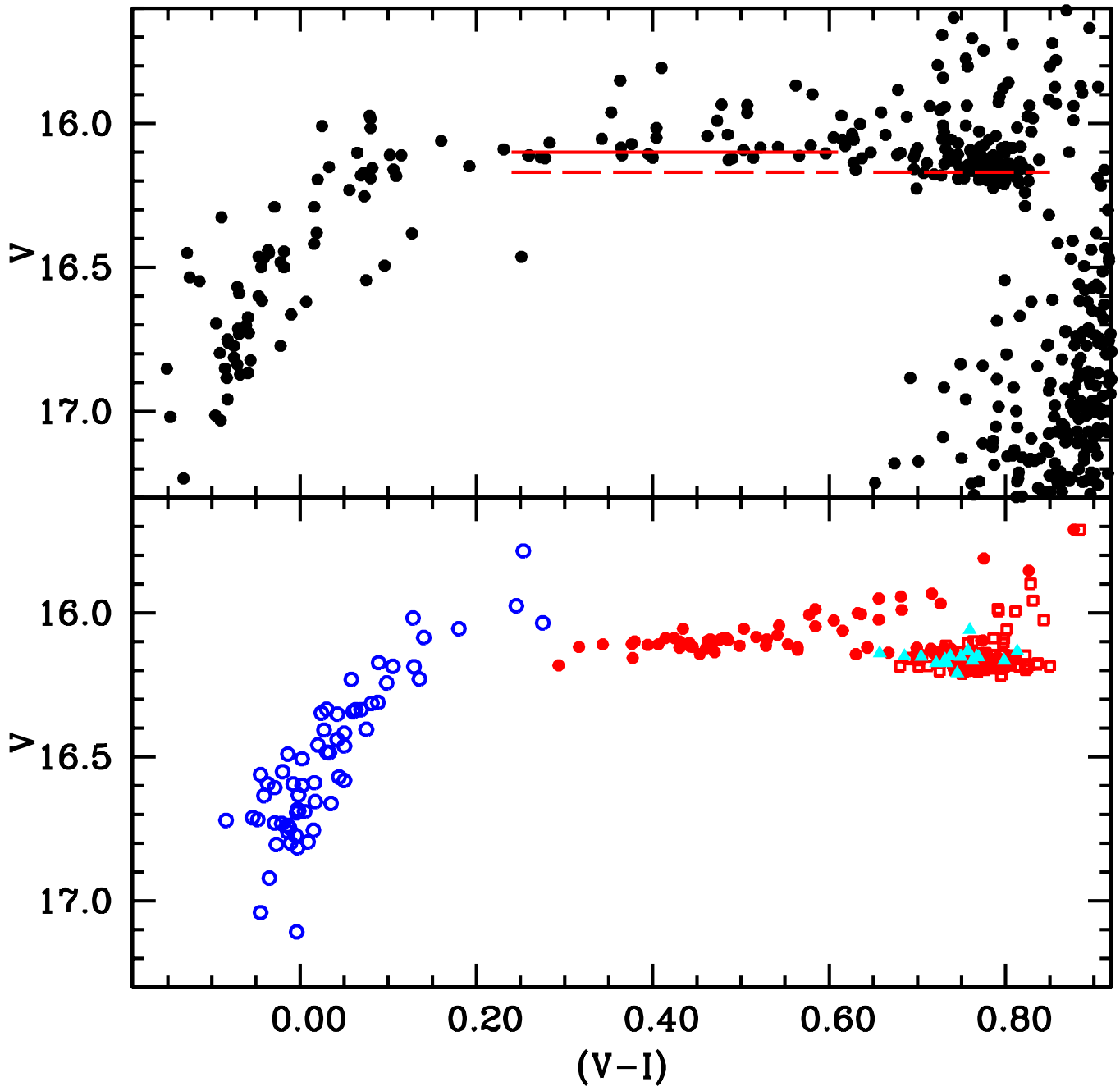

Fig. 8. Comparison between observed (upper panel) and a synthetic HB for NGC 1851. The synthetic CMD has been obtained by considering: $\langle M \rangle = 0.670 \pm 0.005\ M_{\odot}$, $Y = 0.248$ (red open squares); $\langle M \rangle = 0.640 \pm 0.006\ M_{\odot}$, $Y = 0.265$ (filled red circles); $\langle M \rangle = 0.650 \pm 0.004$, $M_{\odot}$, $Y = 0.248$ (cyan filled triangles); $\langle M \rangle = 0.590 \pm 0.005\ M_{\odot}$, $Y = 0.280$ (blue open circles). These populations have been selected in order to reproduce the observed distribution of stars on the HB and SGB, as well as the anomalous red sequence on the RGB in the $(v, (v-y))$ diagram (see text for further details). Solid and dashed lines in the upper panel represent the average brightness of, respectively, the horizontal part of the blue HB and the red HB, as derived from the synthetic CMD. For ease of comparison, the dashed line is also displayed at the colour range of the horizontal part of the blue HB.

Walker (1998) *VI* photometry to create the reference observational CMD, for it includes also mean magnitudes of RR Lyrae stars, that fill the gap seen in Fig. 2 between the RHB and the more extreme BHB. We will denote as 'horizontal part of the BHB' this section of the observed HB.

We have employed as reference set the HB evolutionary tracks for [Fe/H] = −1.31, $Y = 0.248$, [α/Fe] = 0.4 from the BaSTI database[9] (Pietrinferni et al. 2006). In addition, we have interpolated among the α-enhanced BaSTI models at $Y = 0.248$ and $Y = 0.300$, to determine HB tracks for intermediate values of Y, at [Fe/H] = −1.31. Finally, we have also interpolated between the reference set and the CNO and Na anticorrelated models with CNO sum enhanced by 0.3 dex (Pietrinferni et al. 2009) to determine HB tracks with a milder CNO-enhancement, equal to 0.15 dex. We adopted $E(B-V) = 0.02$ (Walker 1998) and employed a distance modulus $(m-M)_V = 15.58$ obtained from matching the mean magnitude of the RHB with our synthetic counterpart.

[9] http://www.oa-teramo.inaf.it/BASTI

In our simulations we have considered as constraints a number ratio between b-SGB and f-SGB stars equal to 70:30, and a 30:10:60 ratio between stars at the blue side, within, and at the red side of the instability strip, respectively. Figure 8 displays a realization of our synthetic calculations of the cluster HB (bottom panel) compared to the observed CMD (upper panel). The number of stars in the synthetic HB is approximately equal to the observed numbers. We considered the observed HB of NGC 1851 formed by the contribution of four different stellar populations, with a Gaussian mass distribution for each component:

- the BHB/f-SGB population: it is associated to the f-SGB and makes up therefore ∼25% of the cluster stellar content. To match both color and magnitude of the BHB we adopted a HB mass of $\langle M \rangle = 0.590 \pm 0.005\ M_{\odot}$ (corresponding to a total mass loss of the RGB progenitor equal to ∼0.20 $M_{\odot}$ for a ∼12 Gyr population with the chemical composition specified below) a normal [C+N+O]/Fe abundance and an helium content $Y = 0.280$ (blue circles in Fig. 8);
- the RHB population: this population is the dominant cluster population (∼55%) and represents the vast majority of the progeny of b-SGB stars. It has been assumed to be ∼1.5 Gyr younger than the BHB one, with a cosmological helium content $Y = 0.248$ and the same [C+N+O]/Fe abundance of the BHB. The observed CMD is reproduced with a HB mass of $\langle M \rangle = 0.670 \pm 0.005\ M_{\odot}$ (open red squares in Fig. 8) consistent with the same total RGB mass loss as for the progenitors of BHB objects;
- the population of Ba-rich stars: this population is ∼10% of the cluster stellar content. It has been reproduced with a mass of $\langle M \rangle = 0.650 \pm 0.004\ M_{\odot}$ (consistent with an intermediate age between the two above populations), assuming a cosmological helium content $Y = 0.248$ and an enhanced [C+N+O]/Fe by 0.15 dex (cyan filled triangles in Fig. 8). This mean mass corresponds to a progenitor age intermediate between the RHB and BHB populations, when the same total RGB mass loss is assumed;
- a fourth population constituting ∼10% of the cluster stars has been added to populate the horizontal part of the BHB visible in Walker (1998) CMD, that includes the instability strip (filled red circles in Fig. 8). We employed for these stars a HB mass of $\langle M \rangle = 0.640 \pm 0.006\ M_{\odot}$, $Y = 0.265$ and normal [C+N+O]/Fe abundances, to reproduce both the color extension and the magnitude of the HB at $0.25 < V-I < 0.55$. Our spectroscopic data do not cover this portion of the HB, but this additional population is obviously necessary to reproduce the observed HB in the region of the instability strip, and accounts for the two Na-rich Ba-poor stars brighter and warmer than the bulk of RHB stars.

Our synthetic HB simulations show that with a suitable choice of age and CNO abundances we can reproduce the location of the Ba-rich stars in the color–magnitude diagram for both RGB and HB stars. Other pairs of parameters are not as successful. The anomalous $v - y$ colours of the RGB Ba-rich stars can only be explained with overabundances of CNO elements. The small differences in luminosity and [Fe/H] rule out pairs such as (He, CNO) or ([Fe/H], CNO).

As outlined above, our selected distribution of initial He abundances generates a satisfactory fit to the overall HB morphology. In particular, the initial He adopted for the bulk of RHB stars and for the horizontal part of the blue HB reproduces nicely the increase of the average HB brightness when

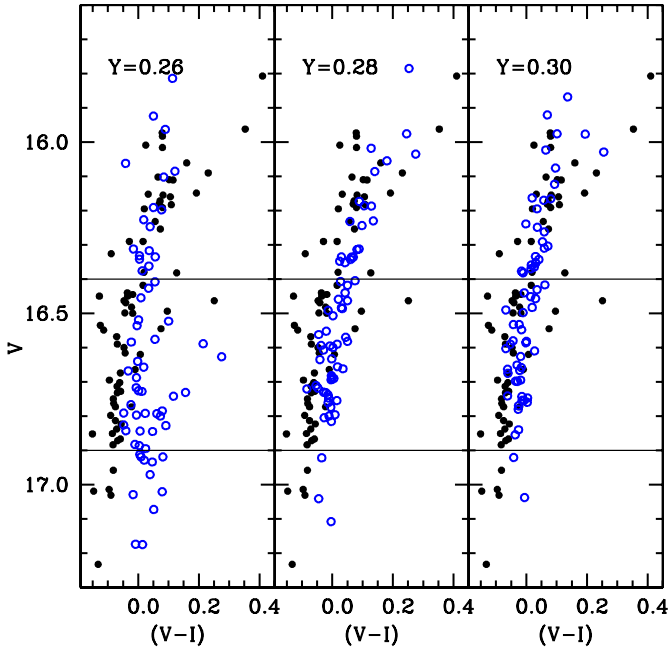

Fig. 9. Comparison between the photometry displayed in Fig. 8 restricted to the bluest HB stars, and the corresponding synthetic HB simulations, for various assumptions about the initial He contents (see labels). The two horizontal lines mark the region in the CMD that include stars whose surface He abundance have been measured for this work.

moving away from the RHB towards higher effective temperatures. On the other hand, as shown by Fig. 9, the bluest HB is almost perpendicular in the $V, (V - I)$ plane, and does not allow a clear-cut selection of the most appropriate initial He abundance. One can safely conclude that the lower He mass fraction $Y = 0.26$ is clearly ruled out, and there is some hint that $Y = 0.30$ generates a too steep sequence compared to the observed CMD, but some constraints are required. They are indeed provided by CMDs that make use of ultraviolet photometric bands, as has been shown conclusively by Busso et al. (2007) and Dalessandro et al. (2011). We have therefore compared our synthetic HB simulations with data in the Strömgren $u, (u - y)$ CMD – obtained from the same dataset used for determining the $T_{\rm eff}$ of our star sample (see the discussion in the previous sections). The comparison is shown in Fig. 10. In this CMD the morphology of the bluer part of NGC 1851 HB puts strong constraints on the initial Y values: both the lower ($Y = 0.26$) and higher ($Y = 0.30$) He abundances are clearly ruled out, whereas an initial He abundance $Y = 0.28$ is able to reproduce the observed distribution of stars in this CMD. This value of Y is consistent with the central value of the He abundance distribution obtained from spectroscopy. Notice the three stars located at $(u - y) < 1.0$, that appear overluminous compared to trend set by the synthetic calculations. Their colors correspond to $T_{\rm eff}$ above 12 000 K, that marks the onset of radiative levitation (Grundahl et al. 1999). It is also important to remark that at the relatively high temperatures of the BHB stars displayed in Fig. 10 the effect of the CNONa abundance anticorrelations on the bolometric corrections to the u and y bands are expected to be negligible (see Sbordone et al. 2011).

This discussion shows that many aspects of NGC 1851 can be derived by using the whole set of observations available for HB stars. However, we acknowledge that we had to consider many different stellar populations, and this may then

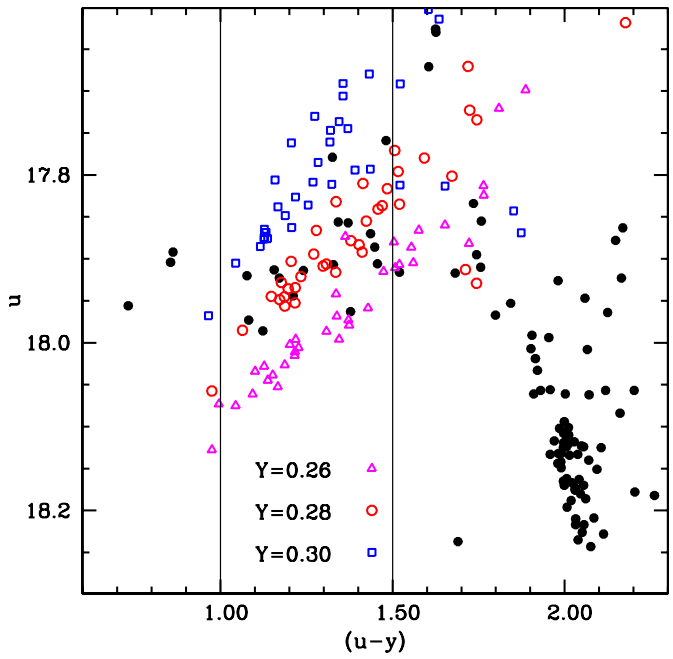

Fig. 10. As Fig. 9 but in the Stroemgren $u,(u-y)$ CMD. The adopted distance modulus and reddening are the same employed in Fig. 8. The two horizontal lines have the same meaning as in Fig. 9.

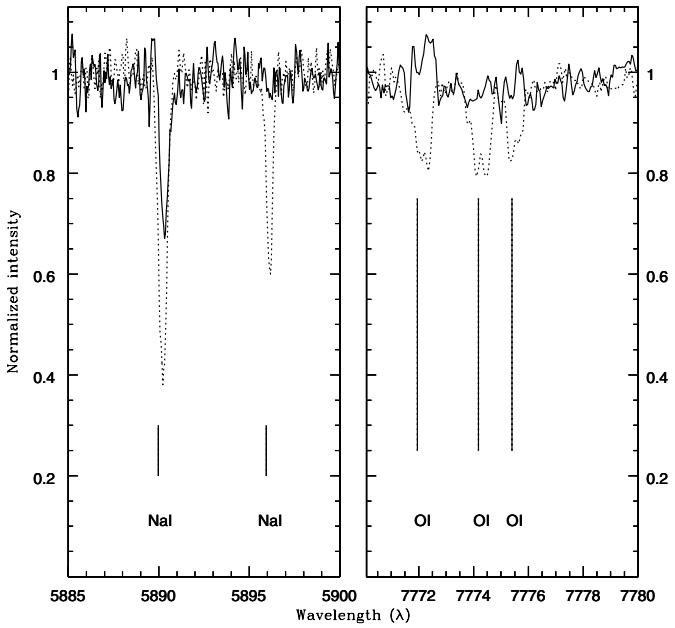

Fig. 11. Comparison between the spectrum of star #46902 (solid line) and that of a star with very similar temperature (#48007, dashed line) in the regions of the Na D (*left panel*) and O I lines (*right panel*). Note that the stellar D1 line at 5890 Å is blended with the interstellar D2 line in these spectra.

appear quite contrived. In addition, we are aware that other combinations of parameters are likely possible, including e.g. suitable mass loss laws for different group of stars. Anyhow, we think that any model trying to reproduce this whole set of observations must assume that NGC 1851 contains many stellar populations and that its history was certainly complex. Finally, we wish to notice that the difference of our derived HB He abundance distribution compared to Salaris et al. (2008) results is mainly due to the different photometric datasets we employed here, as well as to the larger number of observational constraints accounted for in our simulations.

4.6. Peculiar stars

It is very unlikely that stars with radial velocities compatible with that of NGC 1851 are not member of the cluster. For this reason, stars with peculiar abundances should be examined carefully. There are a few such stars. Along the BHB, star #46902 has very low abundances of both O and Na ([O/Fe] = −1.20, [Na/Fe] = −0.56). Other stars of NGC 1851 with a similar temperature have much stronger lines (see Fig. 11); we notice that the Na D2 line is however detectable, and it is not wider than those of other stars, excluding the possibility that this star is a fast rotator. We have not a definite explanation for this anomaly, but it is possible that this is a very metal poor star. This possibility would be most intriguing. We notice that it has a large $u-y$ colour, which might suggest a low gravity.

In addition, a few stars have very high Na abundances. Some examples are shown in Fig. 12. Errors are large for BHB stars, but anyhow star #40227 stands out as peculiar ([Na/Fe] = 1.48). Results for RHB stars are much more robust. There are two RHB stars that have large Na abundances and low Ba-ones. They are warmer and brighter than typical RHB stars. They are then likely stars evolved off the Zero Age HB. Their progenitors were likely RR Lyrae or BHB stars. There is also one star with a very large Na excess (#31903: [Na/Fe] = 0.93). This is a very Ba-rich star. The nature of these extremely Na-rich stars should need a special discussion, that is deferred to a forthcoming paper.

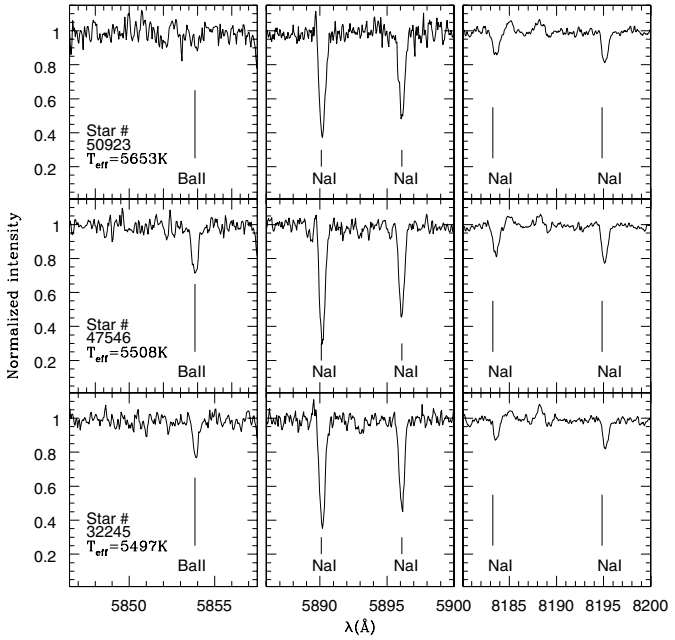

Fig. 12. Comparison between the spectra of three RHB stars: star #50923 is a Na-rich and Ba-poor star; star #47546 is Na-rich and Ba-rich; star #32245 is Na-poor and Ba-poor. Note that the stellar D1 line at 5890 Å is blended with the interstellar D2 line in these spectra.

5. Conclusions

We presented an analysis of the abundances of several elements, including He, N, O, Na, Mg, Si, Ca, Fe, and Ba, in

about a hundred stars along the HB of NGC 1851. We observed 35 BHB stars, 1 RR Lyrae variable, 55 RHB stars, and 13 RGB stars for comparison. Results of this analysis helped to better understand some of the critical issues concerning the formation of this peculiar cluster, which has a bimodal distribution of stars along the HB (about 2/3 RHB and 1/3 BHB), a split SGB (about 2/3 b-SGB and 1/3 f-SGB), and an RGB with a sequence of stars with anomalous $v - y$ colours including some 10% of the stars. The stars in this anomalous RGB are Ba-rich.

The main results we obtained may be summarized as follows:

- RHB stars divide into two groups: the vast majority is Na-poor and O-rich; about 10–15% of the stars are Na-rich and moderately O-poor, most, but not all, of them being Ba-rich.
- These two groups occupy distinct regions of the colour magnitude diagram, the Na-rich stars being redder and slightly brighter than the Na-poor ones.
- An Na-O anticorrelation exists also among BHB stars, that are on average more Na-rich and O-poor than RHB stars. However, there is no clear correlation with temperature/colours.
- The BHB stars are enriched in N, but not exceptionally so. The total CNO abundance is unlikely to be anomalous.
- The He abundance of the BHB is $Y = 0.29 \pm 0.05$. This is consistent with both the cosmological value and a small He enhancement. This confirms the lack of evidence for very large He enhancements within NGC 1851.

When coupled with previous knowledge about this cluster, these results clearly rule out the explanation of the splitting of the SGB as due to variations in the total CNO abundance. A difference in age thus remains the only plausible explanation. On the other hand, we suggest to link the Ba-rich RHB stars with the Ba-rich RGB ones. To explain the anomalous $v - y$ colours, these stars should be very N-rich ([N/Fe] $\sim$ 1.55). This upper limit to the N abundance is not inconsistent with the abundance upper limit of [N/Fe]< 1.55 we obtain for one Ba-rich RHB star.

On the whole, the observational frame suggests that most BHB stars descend from the f-SGB stars and are old while most RHB stars descend from the b-SGB and are young, the difference in age being of the order of 1 Gyr. However, the correlation is possibly not one-to-one: it is in fact possible (though not at all demonstrated) that Ba-rich RHB stars descend from f-SGB stars. If this is the case, then some of the BHB stars and RR Lyrae variables descend from b-SGB stars, else there would be an excess of b-SGB stars with respect to the observed RHB stars. A comparison with the case of NGC 362, a GC with a metallicity and age very similar to that of the young component of NGC 1851, shows that this is not unlikely. In fact, while lacking any evident f-SGB, NGC 362 has a significant population of RR Lyrae variables and a scatter of stars along the BHB. Remarkably, the RR Lyrae of NGC 362 and NGC 1851 are indistinguishable in the period-amplitude diagram (Szekely et al. 2007; Walker 1998), suggesting similar masses and luminosities. The presence of a group of stars that might be identified with the second generation of the young component of NGC 1851 at the cool end of the BHB would contribute explaining the lack of correlations between Na and O abundances with temperature along the BHB.

Several features of NGC 1851 are still unclear. The most relevant is the exact composition (CNO enrichment) and dating of the Ba-rich sequence. This sequence shows evidence for originating from polluters that experienced thermal pulses, and are then likely of rather small mass, but given these uncertainties its role in the formation scenario for this cluster is still to be understood. Progress can be obtained by both a precise determination of the CNO content of these stars and their identification along the SGB of NGC 1851. In addition, the match between the two RGB groups with different Fe abundance found by Carretta et al. (2011a,b) and the evolutionary sequences requires further confirmation and clarification. Finally, the whole scenario for the formation and evolution of this interesting cluster needs to be put on a more sound basis.

Acknowledgements. This publication makes use of data products from the Two Micron All Sky Survey, which is a joint project of the University of Massachusetts and the Infrared Processing and Analysis Center/California Institute of Technology, funded by the National Aeronautics and Space Administration and the National Science Foundation. This research has made use of the NASA's Astrophysical Data System. This research has been funded by PRIN INAF "Formation and Early Evolution of Massive Star Clusters".
We thank Sandro Villanova for having given us access to his unpublished results about CNO abundances in red giants of NGC 1851.

References

Alonso, A., Arribas, S., & Martinez-Roger, C. 1999, A&AS, 140, 261
Alonso, A., Arribas, S., & Martinez-Roger, C. 2001, A&A, 376, 1039
Barklem, P. S., Piskunov, N., & O'Mara, B. J. 2000, A&A, 363, 1091
Behr, B. B., Cohen, J. G., McCarthy, J. K., & Djorgowski, S. G. 1999, ApJ, 517, L135
Behr, B. C., Djorgovski, S. G., Cohen, J. G., et al. 2000a, ApJ, 528, 849
Behr, B. C., Cohen, J. G., & McCarthy, J. K. 2000b, ApJ, 531, L37
Bekki, K., & Yong, D. 2012, MNRAS, 419, 2063
Bellazzini, M., Ibata, R. A., Chapman, S. C., et al. 2008, AJ, 136, 1147
Busso, G., Cassisi, S., Piotto, G., et al. 2007, A&A, 474, 105
Caffau, E., Maiorca, E., Bonifacio, P., et al. 2009, A&A, 498, 877
Calamida, A., Bono, G., Stetson, P. B., et al. 2007, ApJ, 670, 400
Cardelli, J. A., Clayton, G. C., & Mathis, J. S. 1989, ApJ, 345, 245
Carney, B. W., Gray, D. F., Yong, D., et al. 2008, AJ, 135, 892
Carretta, E., Bragaglia, A., Gratton, R. G., et al. 2009, A&A, 505, 117
Carretta, E., Gratton, R. G., Lucatello, S., et al. 2010, ApJ, 722, L1
Carretta, E., Lucatello, S., Gratton, R. G., et al. 2011a, A&A, 533, A69
Carretta, E., Bragaglia, A., Gratton, R. G., et al. 2011b, A&A, 535, A121
Cassisi, S., Salaris, M., Pietrinferni, A., et al. 2008, ApJ, 672, L115
Catelan, M. 1997, ApJ, 478, L99
Catelan, M., Borissova, J., Sweigart, A. V., & Spassova, N. 1998, ApJ, 494, 265
Cyburt, R. H. 2004, Phys. Rev. D, 70, 023505
Dalessandro, E., Salaris, M., Ferraro, F. R., et al. 2011, MNRAS, 410, 694
D'Antona, F., & Caloi, V. 2004, ApJ, 611, 871
D'Antona, F., Caloi, V., Montalban, J., et al. 2002, A&A, 395, 69
Dotter, A., Sarajedini, A., Anderson, J., et al. 2010, ApJ, 708, 698
Fabbian, D., Recio-Blanco, A., Gratton, R. G., & Piotto, G. 2005, A&A, 434, 235
Faulkner, J. 1966, ApJ, 144, 978
Gratton, R. G., Carretta, E., Eriksson, K., & Gustafsson, B. 1999, A&A, 350, 955
Gratton, R., Sneden, C., & Carretta, E. 2004, ARA&A, 42, 385
Gratton, R. G., Carretta, E., Bragaglia, A., Lucatello, S., & D'Orazi, V. 2010, A&A, 517, A81
Gratton, R. G., Lucatello, S., Carretta, E., et al. 2011, A&A, 534, 123
Gratton, R. G., Carretta, E., & Bragaglia, A. 2012, A&ARv, in press
Grundahl, F., & Bruntt, H. 2006, in Chemical Abundances and Mixing in the Milky Way and its Satellites (Springer), 132
Grundahl, F., Catelan, M., Landsman, W. B., Stetson, P. B., & Andersen, M. I. 1999, ApJ, 524, 242
Hanuschik, R. W. 2003, A&A, 407, 1157
Harris, W. E. 1996, AJ, 112, 1487
Kinman, T., Castelli, F., Cacciari, C., et al. 2000, A&A, 364, 102
Korotin, S., Mishenina, T., Gorbaneva, T., & Soubiran, C. 2011, MNRAS, 415, 2093
Kupka F., Ryabchikova T. A., Piskunov N. E., Stempels H. C., & Weiss W. W. 2000, Baltic Astron., 9, 590
Lambert, D. L., McWilliam, A., & Smith, V. V. 1992, ApJ, 386, L685
Lee, Y.-W., Demarque, P., & Zinn, R. 1994, ApJ, 423, L248
Lee, J.-W., Lee, J., Kang, Y.-W., et al. 2009, ApJ, 695, L78
Marino, A. F., Villanova, S., Milone, A. P., et al. 2011, ApJ, 730, L16

Mashonkina, I. I., & Zhao 2006, A&A, 456, 313
Mashonkina, I. I., Shimanskii, V. V., & Sakhibullin, N. A. 2000, Astron. Rep., 44, 790
Mashonkina, L., Korn, A. J., & Przybilla, N. 2007, A&A, 461, 261
Milone, A. P., Bedin, L. R., Piotto, G., et al. 2008, ApJ, 673, 241
Milone, A. P., Stetson, P. B., Piotto, G., et al. 2009, A&A, 503, 755
Pasquini, L., Castillo, R., Dekker, H., et al. 2004, SPIE, 5492, 136
Peterson, R. C., Rood, R. T., & Crocker, D. A. 1995, ApJ, 453, 214
Pietrinferni, A., Salaris, M., Cassisi, S., & Castelli, F. 2006, ApJ, 642, 797
Pietrinferni, A., Cassisi, S., Salaris, M., et al. 2009, ApJ, 697, 275
Piotto, G. 2008, MSAIt, 79, 334
Przybilla, N., & Butler, K. 2001, A&A, 379, 955
Recio-Blanco, A., Aparicio, A., Piotto, G., De Angeli, F., & Djorgovski, S. G. 2006, A&A, 452, 875
Robin, A. C., Reylé, C., Derrière, S.,& Picaud, S. 2003, A&A, 409, 523
Salaris, M., Riello, M., Cassisi, S., & Piotto, G. 2003, A&A, 420, 911
Salaris, M., Cassisi, S., & Pietrinferni, A. 2008, ApJ, 678, L25
Sandage, A., & Wallerstein, G. 1960, ApJ, 131, 598
Sandage, A., & Wildey, R. 1967, ApJ, 150, 469
Saviane, I., Piotto, G., Fagotto, F., et al. 1998, A&A, 333, 479
Sbordone, L., Salaris, M., Weiss, A., & Cassisi, S. 2011, A&A, 534, A9
Skrutskie, M. F., Cutri, R. M., Stiening, R., et al. 2006, AJ, 131, 1163
Sweigart, A. V. 1987, ApJS, 65, 955
Szekely, P., Kiss, L. L., Jackson, R., et al. 2007, A&A, 463, 589
Takeda, Y. 1997, PASJ, 49, 471
van den Bergh, S. 1967, AJ, 72, 70
van den Bergh, S. 1996, ApJ, 471, L31
Ventura, P., Caloi, V., D'Antona, F., et al. 2009, MNRAS, 399, 934
Villanova, S., Piotto, G., & Gratton, R. G. 2009, A&A, 499, 755
Walker, A. 1998, AJ, 116, 220
Yong, D., & Grundahl, F. 2008, ApJ, 672, L29
Yong, D., Grundahl, F., D'Antona, F., et al. 2009, ApJ, 695, L62
Yong, D., Grundahl, F., & Norris, J. 2011, in KraftFest 2011, http://www.ucolick.org/kraftfest/talks/yong_kraftfest.pd